APPLICATION OF THE THIOSULFONATE SWITCH TECHNIQUE AND A MODIFIED BIOTIN SWITCH TECHNIQUE PROTOCOLS TO DETECT PROTEIN *S*-NITROSOTHIOLS IN MOUSE LIVER LYSATES IN 1D AND 2D GEL STUDIES

by

Colin Gregory Miller

A thesis submitted in partial fulfillment
of the requirements for the degree

of

Master of Science

in

Chemistry

MONTANA STATE UNIVERSITY
Bozeman, Montana

July 2015

DEDICATION

This thesis is dedicated to my mom, Melanie Miller, whose unshakable support and constant inspiration has made me the scientist and the person I am today. This thesis is also dedicated to my dear friend Phillip Hartman for always seeing the best in me, even if I could not. I love you both so much and I'm honored to call you my family.

ACKNOWLEDGEMENTS

I would like to acknowledge Dr. Paul Grieco for his support of my research and his guidance through this work. I would also like to acknowledge Drs. Ben Reeves, Ed Schmidt and Brian Bothner for their continued support and collaborations. I've been very lucky to work for all of you. Finally, I would like to thank Mr. Mohammed Refai for his work and support with 2D gels, the staff of the Montana State Department of Chemistry and Biochemistry for their tireless work and Montana State University for giving me this opportunity.

TABLE OF CONTENTS

LIST OF FIGURES

Figure Page

LIST OF FIGURES – CONTINUED

Figure Page

LIST OF FIGURES – CONTINUED

Figure Page

ABSTRACT

While the role of nitric oxide (NO) in cell signaling and liver growth has been well documented, the identification of *S*-nitrosylated proteins, one of the major NO transport mechanisms within the cell, remains a challenge. Classically, the implementation of biotin labeling, known as the biotin switch technique (BST), with streptavidin-agarose bead pulldown and subsequent immunoblotting, has offered the best results for identifying *S*-nitrosocysteine residues within proteins. However, this technique has come under scrutiny for its use of ascorbate as a reducing agent. Numerous published accounts have shown ascorbate's poor reducing potential especially for *S*-nitrosoproteins. To this end, the Grieco lab has shown that pure *S*-nitrosylated proteins can be transformed into *S*-phenylsulfonylcysteine residues, which can be readily converted into mixed disulfides thus allowing for labeling of pure nitrosylated proteins at pH's as low as pH 4. This protocol is referred to as the thiosulfonate switch technique (TST). The Grieco lab has also modified the biotin switch technique to incorporate electrophilic maleimide and orthopyridyl disulfide (OPSS) dyes for fluorescence labeling of the *S*-nitroso proteome. To examine the scope and limitations of the TST vis-à-vis cell lysates, the TST protocol and the modified BST protocol, both employing novel Z-CyDyes developed in the Grieco Laboratory, have been used to specifically label *S*-nitrosylated proteins in complex liver lysates. The successful labeling of mouse liver lysates, employing UV and ascorbate SNO knockout negative controls, is demonstrated in both 1D and 2D gel studies. Also reported herein is the creation of novel second generation maleimide dyes (SO_3-Cy-Mal) based on Z-CyDyes.

S-NITROSOTHIOLS IN PROTEOMIC STUDIES

S-Nitrosothiols

Cysteine (Cys) is the only essential amino acid containing a free thiol and thus is very important in the management of cellular redox activity[1]. Cysteine's slight nucleophilicity, acidic thiol group (pKa ~8), and possession of hybridized p- and d-orbitals allows for the formation of several unique post-translational modifications[2] including disulfide linkages; sulfenic, sulfinic and sulfonic acids; sulfahydryl radicals; persulfides (sulfhydryls) and *S*-nitrosothiols (**Fig 1**.) Protein *S*-nitrosylation is a post translation modification defined as the addition of an NO equivalent to a cysteine thiol (SH) to form an *S*-nitrosothiol (SNO, **Fig. 2**.).

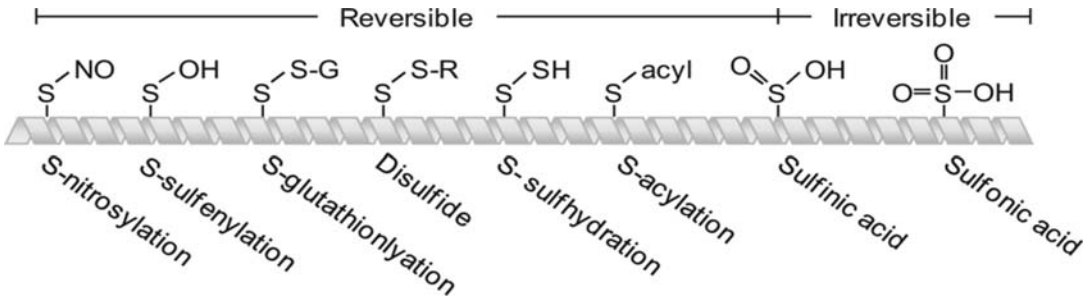

Figure 1. Examples of cysteine modifications. These modifications represent important signaling mechanisms via small molecule transport: *S*-nitrosothiols (NO), sulfenic, sulfinic and sulfonic acids (H_2O_2), glutathionylation (GSH), persulfidation (H_2S.)

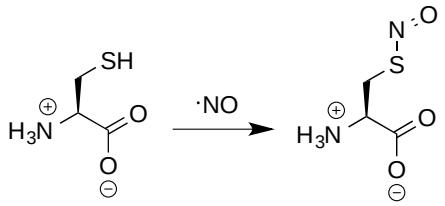

Figure 2. Formation of an *S*-nitrosocysteine residue through the reaction of the cysteine thiol and nitric oxide.

SNO is unique to other cysteine oxidative modifications in several ways: (1) the sulfur-nitrogen bond of SNO bond can undergo both homolytic and heterolytic cleavages, (2) the SNO bond is stabilized by resonance delocalization via two major resonance forms (S-N=O and $^{+}$S=N-O^{-})[3], and (3) the SNO linkage is very labile and can not only be reduced back to a free thiol (SH) or thiyl radical (S•) by loss of an equivalent of NO or NO^{+},[4] but can also transfer NO equivalents between cysteine thiols in a unique reaction called transnitrosation.[5] Transnitrosation represents an important NO transport mechanism and often involves the transfer of nitric oxide to or from the small molecular weight thiols glutathione or cysteine. Protein *S*-nitrosothiols are responsible for nitric oxide (NO) delivery[6] thus playing a significant role in redox biology, regulating enzymatic activity,[7] cell growth and death,[8] vasodilation,[9] modulation[10] and inhibition of prostaglandin synthesis,[11] glutamate-dependent neurotransmission,[12,13] and G-protein-coupled receptor signaling.[14,15] Aberrant *S*-nitrosylation has been implicated in several disease states including neurodegeneration,[16] cardiopulmonary stress,[17] skeletomuscular disease,[18] and tumor initiation and growth.[19] However, due to the lability of *S*-nitrosothiols, much is still unknown about this post-translational modification, especially regarding its selectivity and functionality. For these reasons, the investigation of the *S*-

nitrosoproteome has recently been given significant attention. The thiosulfonate switch technique (TST),[20,21] the modified biotin switch technique (unpublished results from the Grieco laboratory, *vide infra*), and the BST[22] represent valuable protocols for mapping this proteome *in vivo*.

The major source of cellular *S*-nitrosothiols are the nitric oxide synthases (NOSs) which convert L-arginine to L-citrulline using NADPH, tetrahydrobiopterin, and oxygen which generates NO as a byproduct.[23] NOSs are categorized by their three major isoforms: neuronal (nNOS or NOS1), inducible NOS (iNOS or NOS2) and endothelial (eNOS or NOS3.) Protein interactions with NOSs provide for a certain aspect of specificity for the generation of *S*-nitrosothiols, as is seen with the interaction of iNOS and cyclooxygenase-2.[24] Recent work[25] has shown that eNOS binds specifically to multiple proteins associated with the regulation of *B*-adrenergic receptor trafficking, indicating eNOS nitrosylates specifically rather than indiscriminately binding multiple targets.

Formation of *S*-nitrosothiols intercellularly is usually accomplished through reaction of a cysteine thiol with one or more nitrosants (**Fig. 3**), most common of which is peroxynitrite (ONOO-), the product of ·NO and superoxide $O_2^{-}\cdot$. Superoxide is released as a byproduct of several enzymes, including NADPH oxidase and Complexes I and III of the mitochondrial electron transport chain. Superoxide is one of the major cellular species related to oxidative stress.[24]

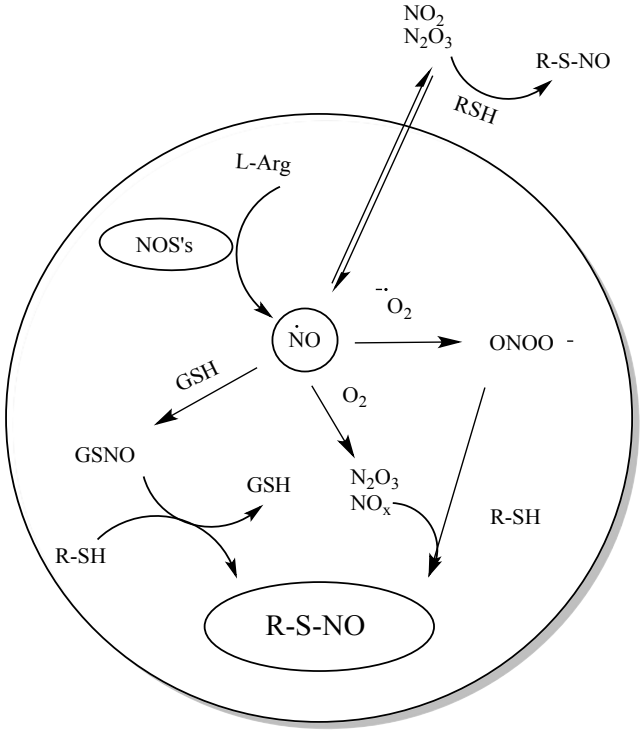

Figure 3. Intercellular and extracellular sources of NO stress

Proteomics

Proteomics is defined as the comprehensive study of a specific proteome including protein abundance, various modifications, and protein-protein interactions/protein networks to help better understand cellular processes.[25] Due to the lability of •NO and *S*-nitrosothiols, a static view of the proteome doesn't fully define the cellular functions taking place. Looking at *S*-nitrosylation from the dynamic viewpoint emphasized in proteomics allows for not only quantification and identification of SNO proteins, but also facilitates understanding of the diverse role of NO, NOSs and SNO target proteins and how these interact under various disease states. Sodium dodecyl

sulfate polyacrylamide gel electrophoresis (SDS-PAGE) and specifically two dimensional difference gel electrophoresis (2D-DIGE) are techniques that offer high specificity, accuracy and throughput and thus have been a cornerstone of proteomic studies in protein up/down regulation.

2D-gel electrophoresis separates proteins orthogonally by two criteria; first, proteins are separated by their isoelectric point (PI) and second, by their size. Separated proteins can be excised and extracted from the gel matrix for further analysis, such as mass spectrometry. Prior to 1997,[28] multiple proteins samples could not be run on a single gel, limiting comparative analysis of a proteome. However, with the development of 2D-DIGE, multiple samples can be run on a single gel by employing fluorescent dyes; each protein sample i.e. control, internal standard, or experimental, is labeled with a different fluorescent dye each fluorescing at a unique wavelength, thus each sample is measured individually and protein abundance can be determined in relationship to the other samples. This technique is referred to as multiplexing.

The standard dye families chosen for multiplexing experiments are most often a variation of the cyanine dyes, or CyDye. CyDyes have several distinct advantages compared to other probes. First, each of the CyDyes, Cy2, Cy3 and Cy5, have the same approximate molecular mass, so a protein labeled with a Cy2 adduct should have the same overall mass as that same protein labeled with a Cy5 adduct. This becomes especially important when multiple samples are run on the same gel; because the protein adducts are the same mass, labeled proteins from one CyDye can be directly compared on the same gel to proteins labeled with another CyDye. Furthermore, each of the three dyes

has similar reactivity and solubility and form stable dye adducts to proteins without significantly affecting conformation. However, overall solubility of the CyDyes was poor and the positively charged cyanine core of the dye could alter protein pI. This issue was addressed with the Grieco lab's synthesis of the Z-CyDye families. The Z-CyDyes, bearing a negatively charged cysteic acid chain, have zwitterionic character and thus have higher solubility in water compared to the more nonpolar CyDyes and also have a smaller affect on protein pI.[29]

A Z-CyDye family of probes has already been utilized in multiplexing proteomics in the study of the thermophillic archaea *Sulfolobus solfataricus* (**Fig. 4**.) Using NHS-ester modified zwitterionic cyanine dyes, the total soluble protein of *S. Solfataricus* was labeled. NHS functionalized dyes react specifically with lysine residues, an amino acid present in almost all proteins. As will be reported in this thesis below, the use of multiplexing has been of particular use in the identification of *S*-nitrosothiols using a newly developed protocol called the thiosulfonate switch technique (TST)[20] as well as a modification of the biotin switch technique (BST), both developed in the Grieco laboratory. It's important to note that the original BST was developed by Jaffrey *et al* in 2001.[22]

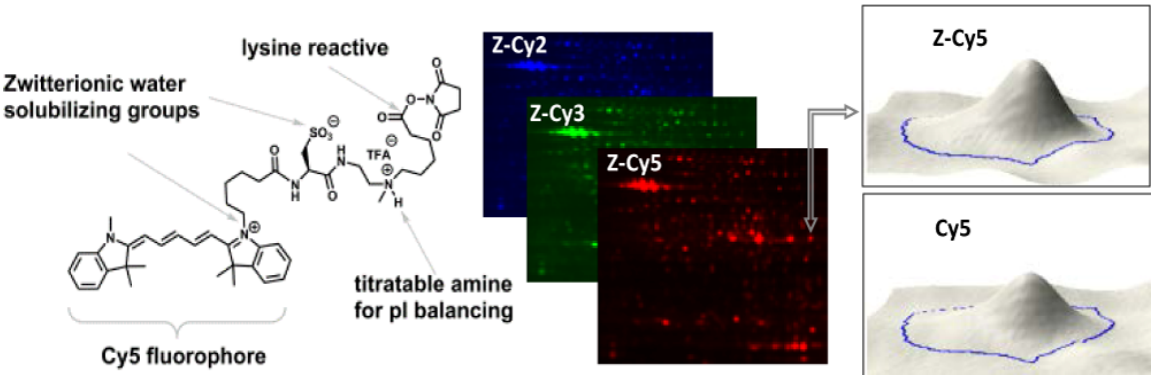

Figure 4. Multiplexing experiment to label *S. Solfataricus* with the Z-Cy-NHS dye set[29]

Use of multiplexing has been of particular use in the identification of *S*-nitrosothiols, *vide infra*. A sample with all *S*-nitrosothiols reduced by either a UV photolysis or ascorbate reduction knockout control sample can be run on the same gel as a nitrosylated SNO sample, i.e. a sample *S*-nitrosylated by common nitrosant such as *S*-nitroso-*N*-acetyl-penicillamine (SNAP,) *S*-nitrosocysteine (SNOC,) or *S*-nitrosoglutathione (GSNO) could be labeled with Z-Cy5, a sample with all SNO eliminated prior to labeling with the addition of ascorbate could be labeled with Z-Cy3 and an internal standard derived by combining knockout and nitrosylated samples could be labeled with Z-Cy2. Thus, all these samples could be combined, run on the same gel and imaged with separate wavelengths to measure each individual condition. To accomplish these goals, new families of Z-CyDyes have been developed by the Grieco laboratory for both the TST and modified BST protocols; a thiol reactive Z-Cy-SH was synthesized for the TST protocol (**Fig. 10** , Chapter 1) and electrophilic OPSS (**Fig. 18**) and maleimide **(Fig. 19**) Z-CyDyes dyes for the modified BST protocol.

S-Nitrosothiol Quantification Techniques

Originally, *S*-nitrosylation could only be measured by its total content within the proteome. Due to the reactivity of the S-NO bond, early strategies relied on the liberation of NO or NO_2^-, which were classified as NO-based detection methods, the most common of which involves use of the Hg^{2+} ion to heterolytically cleave the S-NO bond, forming a mercury-thiol complex and liberating an equivalent of the nitrosonium ion (NO^+) which rapidly hydrates to NO_2^-, a potent nitrosant.[30] Several chemiluminescence techniques, including the Griess-Saville assay,[31] are based upon this reaction; NO^+ reacts with sulfanilamide to form a diazonium salt, to which an organic molecule such as N-(1-napthyl)-ethylenediamine or 4,5-diaminofluoresceine (DAF) is added to form a fluorophore which can be detected by UV-Vis spectroscopy. Other quantification techniques depend on the reduction of *S*-nitrosothiols by ultraviolet light or a chemical reductant such as tri-iodide and the subsequent reaction of NO with ozone to emit light.[30] Limits of detection for these techniques vary between 500nM (Griess-Saville) to 2pM (ozone chemiluminescence), however, these techniques lack the ability to identify which proteins are *S*-nitrosylated and at what cysteine residues the modification has occurred. In order to fully understand the role of NO and its protein interactions, a technique capable of labeling *S*-nitrosylated thiols is necessary. Such a method was realized by the biotin switch technique (BST) by Jaffrey *et al* in 2001.[22]

The BST was the first technique to target the cysteine thiol rather than the NO released and subsequently became the standard method for SNO detection. Since 2001, the BST has been modified to compliment other techniques, leading to increased

sensitivity and throughput. Other techniques in combination with the BST include resin assisted capture (SNO-RAC), tryptic digests (SNO-SID) and the combination of the two (SNO-RAC with on-resin digestion). Despite the many variations of the BST, all share the basic three step protocol that defines the biotin switch assay (**Fig. 5**): 1) blocking of free thiols by *S*-methyl methanethiosulfonate (MMTS), 2) ascorbate reduction of the S-NO bond to form thiolate (S^-) and *O*-nitrosoascorbate and 3) labeling of cysteine thiols with (N-[6-(biotinamido)hexyl]-3'-(2'-pyridyldithio)propionamide) (biotin-HPDP, **Fig. 6**) or similar affinity tag (thiopropyl sepharose for resin assisted capture). Biotinalated proteins can be pulled down with streptavidin agarose beads to separate biotinylated proteins from unlabeled proteins followed by elution using an acidic solution (acetic acid or formic acid) to maintain the S-S-biotin linkage or with a reducing agent such as dithiothreitol (DTT,) to leave a free thiol (SH) on the protein. The BST has also been paired with resin assisted capture (RAC) columns and mass spectrometry to enrich and identify *S*-nitrosylated proteins and peptides in complex lysates. Nitrosylated proteins, after blocking and ascorbate reduction, are captured on the RAC column and purified to give only NO protein.

While the BST has become the standard method for SNO detection, numerous questions have been raised concerning its accuracy due in part to the use of ascorbate to reduce *S*-nitrosothiols. Previous workers[20,33,34] have shown that ascorbate is a poor reducing agent and that its efficiency is greatly compromised when the targeted *S*-nitrosocysteine residue is buried or inaccessible.

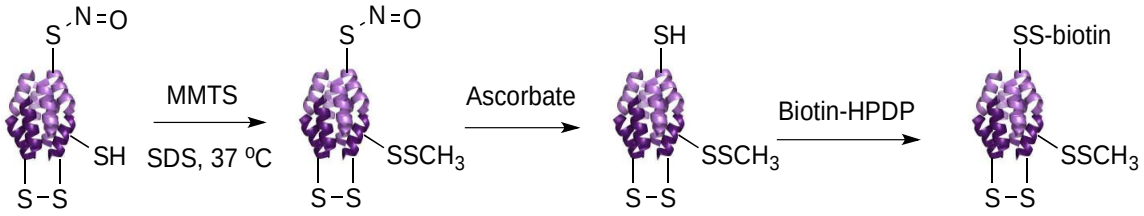

Figure 5. Overview of the biotin switch technique (BST) with biotin-HPDP probe.

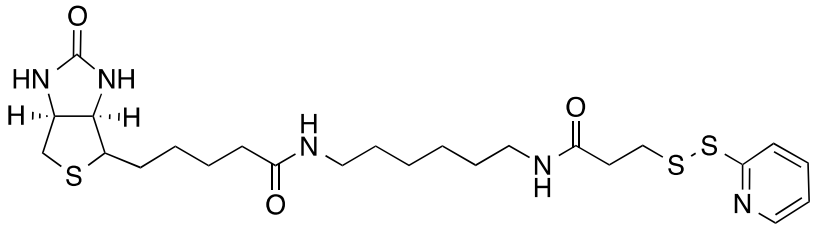

Figure 6. Structure of Biotin-HPDP

Furthermore, the product of ascorbate reduction of SNO, *O*-nitrosoascorbate, is itself an NO donor and can release NO at physiological pH within minutes of its formation. Finally, concerns have been raised regarding ascorbate's interaction with disulfides. In the presence of metal chelators or UV light, the semi-dehydroascorbate radical can be produced which reduces the disulfide of biotin-HPDP, which can undergo thiol-disulfide exchange with MMTS blocked thiols, leading to false positives. These claims were investigated by Foster and Stamler *et al*[35] and Zhang's findings were largely discredited due to the assay being conducted with exposure to indirect sunlight, promoting the ascorbate radical formation. However, it is clear that the specificity of the BST is compromised by ascorbate both due to its poor reducing ability and its possibility for thiol-disulfide exchange.

A recent report[36] in the literature details the development of a detection technique without the reliance on ascorbate reduction. Of the many techniques for SNO detection, Ischiropoulos' organo-mercury based technique has shown the most promise. This technique relies on the high affinity of phenyl mercury for *S*-nitrosothiol cysteines. The protocol (**Fig. 7**), like the biotin switch technique, requires initial blocking of free thiols employing MMTS, iodoacetamide (IAM), or *N*-ethylmaleimide (NEM). Subsequent addition of an organomercury resin displaces NO and forms a stable S-Hg-Probe adduct. Ischiriopoulos' protocol selectively retains the thiols from the *S*-nitrosothiols (and any unblocked free thiol), which can later be eluted to give concentrated SNO proteins or peptides.

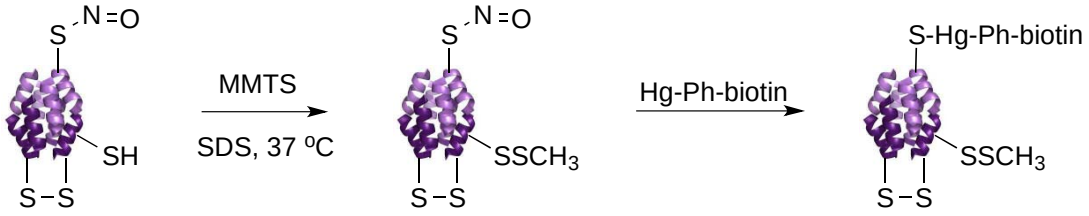

Figure 7. Overview of the organomercury based switch assay with phenylmercury-biotin

The need for a non-toxic (mercury free) protocol that eliminates the use of denaturing agents and heat that is capable of accurately mapping the SNO proteome remains an important problem. To address this pressing issue, the Grieco group developed the novel thiosulfonate switch technique, which uses benzensulfinic acid to convert SNO residues to *S*-phenylsulfonylcysteine residues at low pH.[20] This protocol, which eliminates the use of ascorbate and SDS, is thought to be capable of labeling SNO residues even in buried sites.

As with the BST, the thiosulfonate switch involves a three step protocol; 1) blocking of free thiols with *S*-phenylsulfonylcysteine (SPSC) thus converting a SCys group into an SSCys residue, 2) conversion of *S*-nitrosothiols to *S*-phenylsulfonylcysteine residues with sodium benzenesulfinate and 3) displacement of the benzenesthiosulfonate with a dye probe, resulting in a fluorescently labeled mixed disulfide linkage (**Fig. 8**). Originally, this protocol was performed with a zwitterionic rhodamine-SH probe (**Fig. 9**,) but has since been labeled with a 3-color Z-Cy-SH probe set (**Fig. 10**) (*vide infra*).

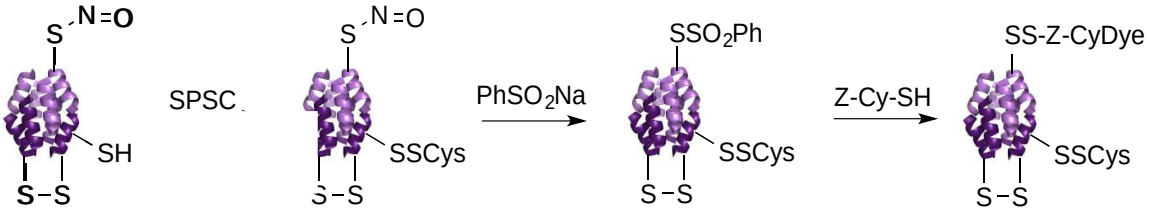

Figure 8. Overview of the thiosulfonate switch technique using accompanying Z-Cy-SH dyes as labeling probes.

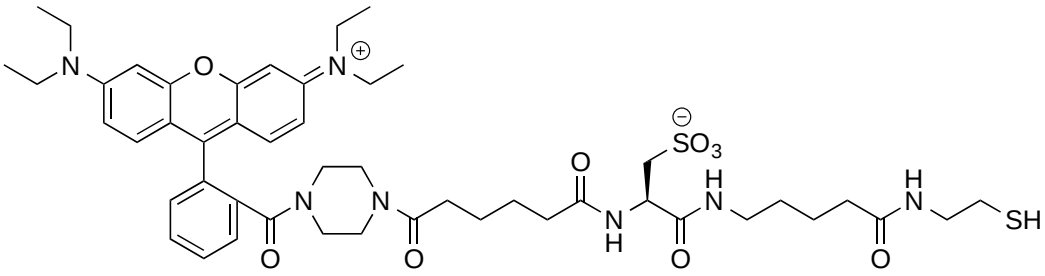

Figure 9. Structure of the zwitterionic Rhod-SH probe used with the TST protocol.

The reaction of benzenesulfinic acid in sulfuric acid with GSNO and *S*-nitrosocysteine at pH 1 has been known for some time.[37] However, these conditions are not compatible with the use of proteins due to solubility issues. Studies by Grieco *et al,*[21]

have shown that the optimal pH for trapping of *S*-nitrosothiols is pH 4. The byproduct of this reaction, $PhSO_2NHOH$, also known as Piloty's acid, is stable at pH 4 and is a poor NO donor, unlike *O*-nitrosoascorbate. Another advantage of the TST stems from its being conducted at a low pH, thus minimalizing the possibility of thiol-disulfide and NO exchange. The rate constant of the TST reaction was shown to be on the same order as the BST, ~0.041 M^{-1} s^{-1}. However, in contrast to the TST which is conducted at low pH, the BST works well only at high pH relative to physiological pH.

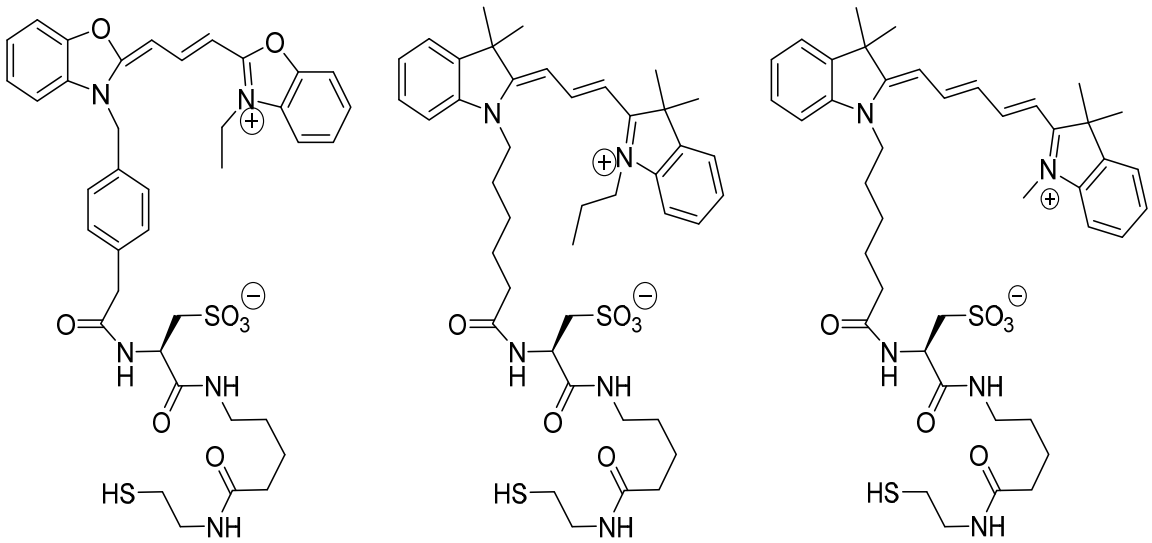

Figure 10. Structures (from left to right) of Z-Cy2-SH, Z-Cy3-SH and Z-Cy5-SH dyes used with the TST protocol

THE THIOSULFONATE SWITCH TECHNIQUE

Conversion of *S*-phenylsulfonylcysteine Residues to Mixed Disulfides at pH 4.0

The TST protocol requires a mild acidic pH to convert SNO into *S*-phenylthiosulfonates. Unlike the BST protocol and other equivalent techniques which employ physiological pH or higher pH, the TST protocol is conducted at pH 4.0 in order to retain the thiol redox state and minimalize disulfide exchange and transnitrosation. To demonstrate the retention of the thiol redox state, the absorbance of 10 mM GSNO (λ_{max} = 545nm, $\varepsilon = 15M^{-1}\ cm^{-1}$, $n_N \rightarrow \pi^*$) in pH 4.0 ammonium formate buffer was monitored over 50 min with and without the reductant DTT (10mM.) This experiment was repeated at pH 4.8, 5.5 and 7.0. While there was minimal decrease in absorbance at pH 4.0 and 7.0 with no DTT present, the GSNO absorbance in the presence of DTT decreased rapidly as the pH increased (**Fig. 11**). At pH 4.0, only a 1% difference between the presence and absence of DTT was noted, however at pH 4.8, 5.5 and 7.0, the % differences were 17%, 47% and 75% (respectively). This data in consistent with other literature reports showing an increase in transnitrosation rates at elevated pH. This data also demonstrates the obvious advantages of a proteomic study carried out at pH 4.0.

The Grieco lab had initially reported the successful conversion of *S*-nitrosoglutathione into the corresponding *S*-phenylthiosulfonate, $GSSO_2Ph$, but had yet to demonstrate the successful displacement of the *S*-phenylthiosulfonate linkage with a fluorescent probe. The successful conversion of an *S*-phenylthiosulfonate linkage with a fluorescent probe has recently been reported from the Grieco Laboratory.[20]

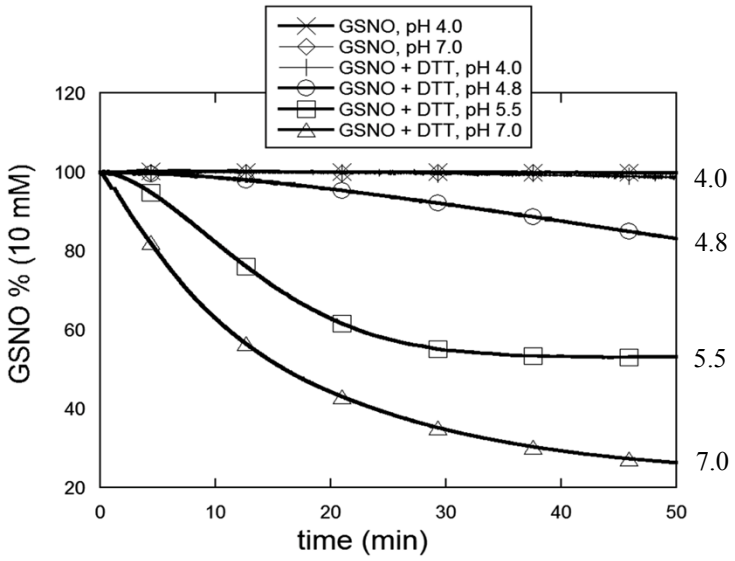

Figure 11. Reduction of GSNO (as % GSNO) over time (min) at varying pH's with and without equimolar DTT.

$GSSO_2Ph$, the *S*-phenylthiosulfonate product of GSNO and benzenesulfinic acid, was added to a reactive rhodamine fluorophore bearing a thiol probe, Rhod-SH **(Fig. 9**). The expected product, Rhod-SSG, was 95% pure with 5% Rhod-SH present by reverse phase HPLC trace with detection at 562nm. No such adduct was observed when $GSSO_2Ph$ was replaced with GSH or GSSG, only the Rhod-SH probe was detected, confirming that the thiol reactive probes undergoes rapid exchange of the *S*-phenylthiosulfonate adduct at pH 4.0, but does not exchange with free thiol (GSH) or disulfides (GSSG.)

Commercially available blocking agents such as IAM, NEM and MMTS were originally considered for the thiol blocking step of the TST. However, it was shown that these thiol blockers were unsuccessful at pH 4.0, thus a new blocking agent was required. The thiosulfonate adduct from reaction of *S*-nitrosocysteine with benzenesulfinic acid, Cys-SSO_2Ph or *S*-phenylsulfonylcysteine (SPSC), was chosen as the blocking agent.

While the reaction of SPSC at basic pH (0.1 M sodium bicarbonate) had been well documented,[36] its blocking potential at mildly acidic pH's had been unreported. Additionally, SPSC's efficiency as a thiol blocker had not been compared to well-known, commercially available blocking reagents such as MMTS, NEM, and IAM. Finally, the reaction of SPSC with disulfides had not been assessed for the potential of disulfide exchange. The reaction of SPSC at pH 4.0, in the presence of GSSG and $(Gly\text{-}Cys)_2$, showed no product formation after 1 h. SPSC's thiol blocking potential was determined vs MMTS, NEM and IAM by reacting each with Rhod-SH. SPSC reacted faster than the three other blocking reagents with approximately full conversion in 1 min. Comparatively, MMTS had only 22% conversion in 1 min and 97% conversion at 30 min, NEM showed 48% conversion after 1 h and IAM showed no conversion after 1 h. This experiment indicates that both MMTS and SPSC are efficient blocking agents at pH 4.0, but that SPSC is the more effective thiol blocker for the TST protocol.

Further assessment of the blocking potential of SPSC was examined by its reactions with several biologically relevant thiols of varying pK_a's. 2 mM solutions of penicillamine, glutathione and captopril, with pK_a's of 7.9, 8.8 and 9.8 respectively, were subjected to the blocking conditions with SPSC (1.8 mM) employing pH 4.0 buffer for 2 min and analyzed by reverse phase HPLC with UV-Vis detection at 265 nm [λ_{max} of SPSC (R_t = 10 min) and $PhSO_2Na$ (R_t = 12 min)]. Trace analysis showed complete conversion of SPSC to $PhSO_2Na$ for both penicillamine and glutathione and 87% conversion for captopril, **Fig. 12**, meaning that SPSC is capable of readily blocking thiols

of varying pKa's at low pH and thus doesn't require formation of the deprotonated thiolate for conversion.

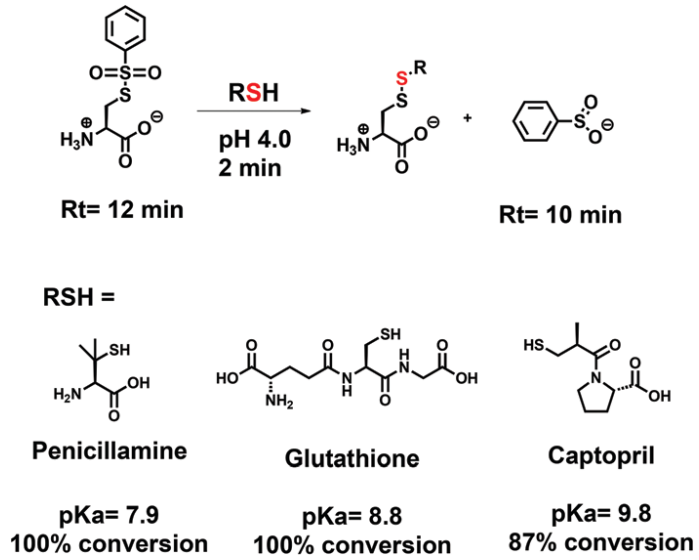

Figure 12. Blocking of thiols with varying pKa's using SPSC

To assess the scope and limitations of applying the TST protocol to protein *S*-nitrosothiols, a number of experiments were undertaken employing *S*-nitroso bovine serum albumin (BSA-SNO.) BSA contains only one free thiol (Cys 34) and is commercially available and known to form a stable *S*-nitrosothiol (BSA-SNO.) A mixture of BSA-SNO and BSA, with varying amounts of BSA-SNO (0.0, 0.15, 0.3, 0.6, 1.2 and 1.8 µg) to give total protein of 6.6 µg for each sample, was labeled by the TST protocol. Samples were treated with SPSC (0.8 nmol, 1h), $PhSO_2Na$ (2.5 µmol, 30 min) followed by Rhod-SH (20 nmol, 10 min). These samples were run on 1D SDS-PAGE non-reducing gels and fluorescent imaging of the gel was done using a GE Typhoon Trio scanner. Because BSA has only a single free thiol, the linear relationship between spot

volume and BSA-SNO (μg) shown in **Fig. 13** indicated that only the *S*-nitrosothiol was labeled. This is further supported by the accompanying coomassie stains that show normalized amounts of protein for each lane.

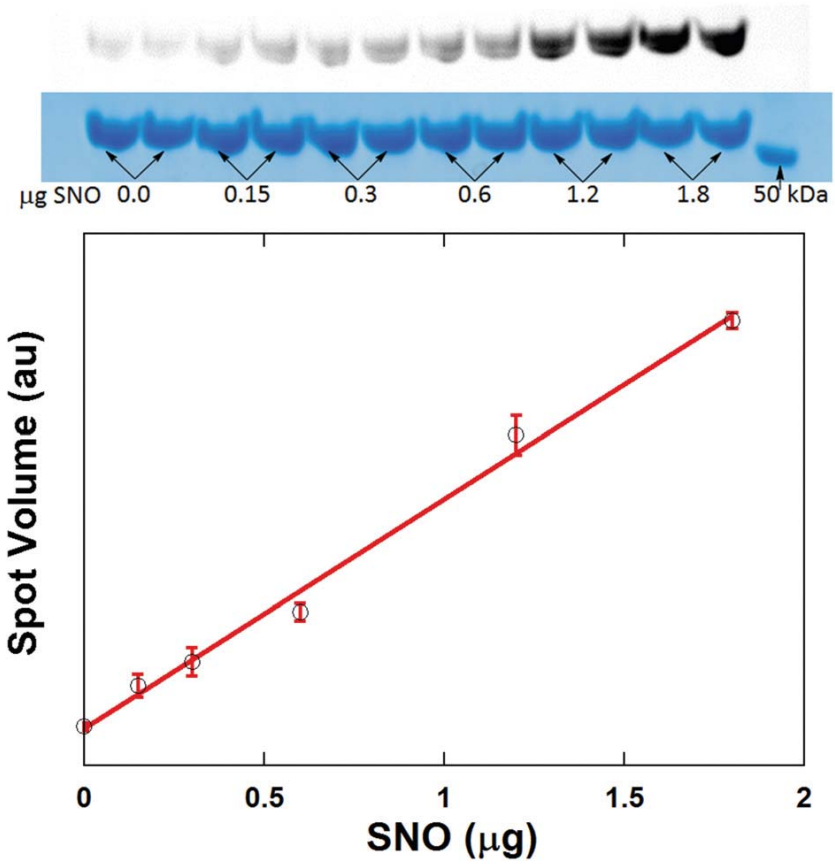

Figure 13. Spot volume vs. μg BSA-SS-Rhod from fluorescence image of 1D nonreducing SDS-PAGE gels. Accompanying coomassie stain shows equivalent amount of protein in each lane.[20]

AdhR*, a C-terminally truncated and functional variant of AdhR (alcohol dehydrogenase regulator, from *Bacillus subtilis,*) is a regulatory enzyme with an active-site thiol (Cys52). It has been shown that upon nitrosylation (GSNO, 10 eq., 25 mM HEPES, 400 mM NaCl, 1 mM EDTA, 0.1 mM bathocuproine disulfonate, pH = 7.0, 1 h)

AdhR* gives rise to AdhR*-SNO (53% SNO, 47% AdhR*-SH.) Interestingly, AdhR*-SNO resists ascorbate reduction, vide infra. Thus, upon subjecting the above mixture of AdhR*-SNO and AdhR*-SH to ascorbate reduction (20 mM, pH 7.5 HEN (100 mM HEPES, 1mM EDTA, 0.1 mM neocuproine) buffer) for 1 h, at ambient temperature, in the dark (**Fig. 14** solid line), there is almost no visible reduction of AdhR*-SNO relative to AdhR*-SH, based upon the presence of AdhR*-SNO in the deconvoluted mass spectra after 1 h of ascorbate reduction. The lack of reduction of AdhR*-SNO by ascorbate in this experiment is yet another example of ascorbate's inability to reduce SNO. It is likely that reduction of AdhR*-SNO to AdhR*-SH could be achieved utilizing denaturing agents (such as SDS) with heat and additional time, however, these conditions dramatically affect the thiol redox state of the sample. This redox state becomes more important as more complex protein and cellular environments are analyzed.

To further demonstrate the selectivity of the thiosulfonate switch technique protocol towards *S*-nitrosothiols, a mixture of BSA-SNO and AdhR*-SH (50 μM each, 5 μg of each pure protein) was labeled using the TST protocol. ESI-TOF analysis, **Fig. 15**, of the labeled mixture showed that while BSA-SNO was detected as the thiosulfonate switch adduct (BSA-SS-Rhod, 67,376 amu,) the AdhR*-SH was only detected as the blocked thiol adduct (AdhR*-SS-Cys, 14,557 amu.) This indicates that only *S*-nitrosylated BSA was labeled with the fluorescent probe and the free thiol of AdhR*-SH, blocked with SPSC, yielded no dye-labeled protein adduct. This experiment was repeated for BSA and AdhR*-SNO (53% SNO, 47% free thiol) and showed similar results. The

free thiol BSA was only detected by ESI-TOF, **Fig. 16**, as the thiol blocked adduct (BSA-SS-Cys, 66,549 amu,) while no fluorescent dye adduct was observed.

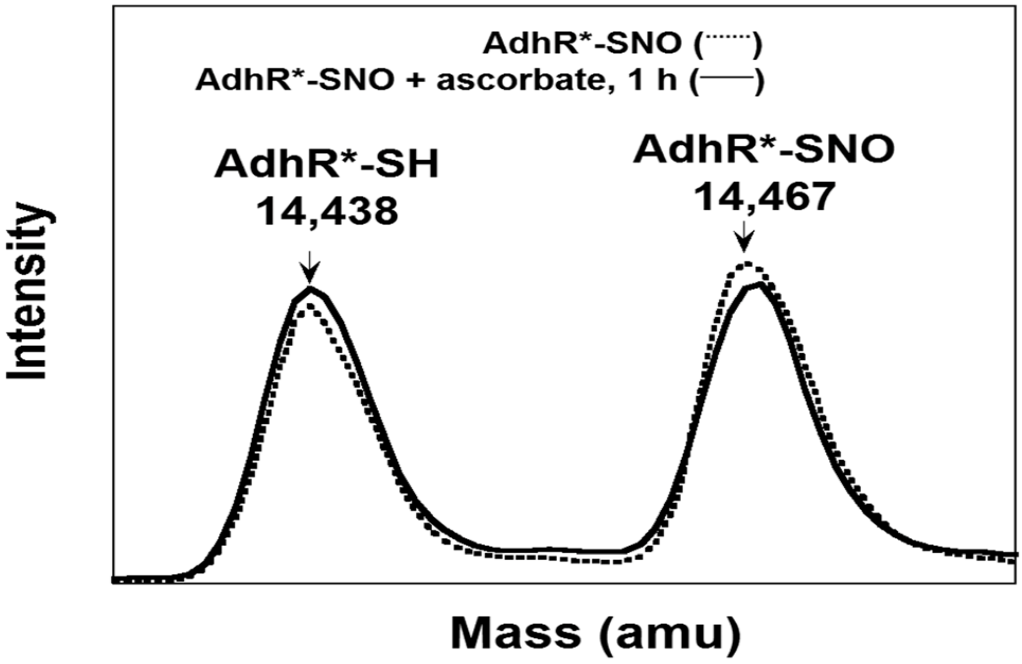

Figure 14. Deconvoluted mass spectra of AdhR*-SH and AdhR*-SNO before ascorbate reduction (dotted line) and after the addition of 20 mM ascorbate (solid line.)[20]

The detection of both the blocked thiol adduct of AdhR*-SH (AdhR*-SS-Cys, 14,557 amu) and the dye labeled thiol adduct of AdhR*-SNO (AdhR*-SS-Rhod) was expected due to the roughly 50% free thiol composition of the AdhR* mixture.

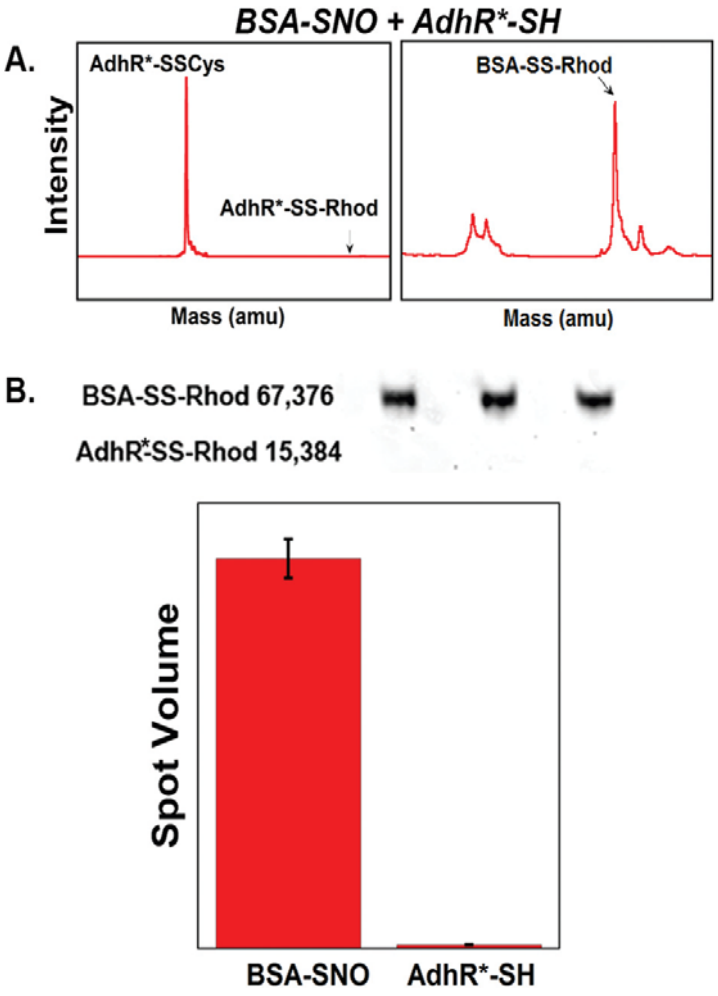

Figure 15. (A) Deconvoluted mass spectra of the target proteins AdhR*-SH (as blocked thiol AdhR*-SS-Cys) and BSA-SNO (as labeled protein BSA-SS-Rhod.) (B) Fluorescence gel image of labeled protein mixture run on 1D nonreducing SDS-PAGE gels. Spot volumes of the labeled proteins calculated in ImageJ.[20]

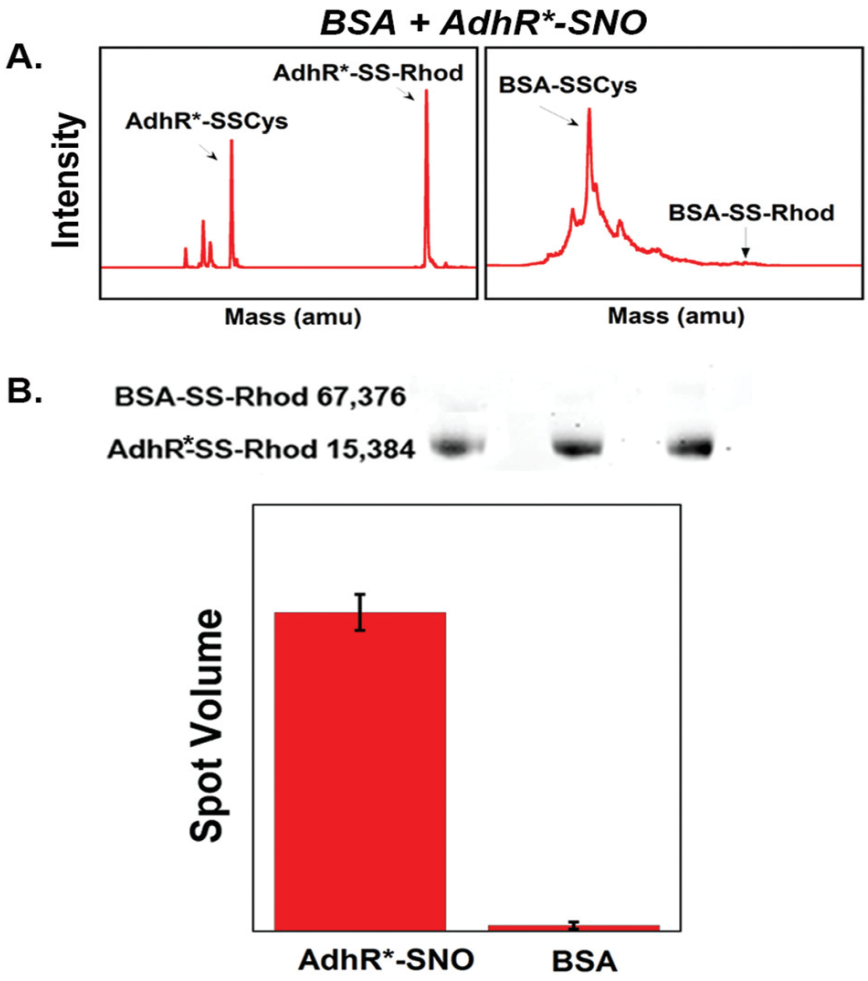

Figure 16. (A) Deconvoluted mass spectra of the target proteins AdhR*-SNO and AdhR*-SH (as labeled thiol adduct AdhR*-SS-Rhod and blocked thiol AdhR*-SS-Cys) and BSA (as blocked thiol BSA-SS-Cys.) (B) Fluorescence gel image of labeled protein mixture run on 1D nonreducing SDS-PAGE gels. Spot volumes of the labeled proteins calculated in ImageJ.[20]

Application of the TST Protocol to Mouse Liver Lysates: 1D Gel Analysis

The TST had been successfully demonstrated in the labeling of *S*-nitrosothiols in two-protein samples. As expected, the TST showed minimal false labeling with the inclusion of the thiol blocker SPSC. In order to further assess the scope and limitations of

the TST, it was imperative to examine the efficacy of the TST on lysates. To this end, mouse livers, obtained from Dr. Ed Schmidt, Department of Microbiology and Immunology, Montana State University, were lysed and subjected to *S*-nitrosylation [200 nmoles GSNO in pH 8.0 HEN buffer for 200 μg protein, 1 h, dark, ambient temperature]. The use of 312nm UV was chosen as a negative SNO-knockout control, rather than ascorbate due to the poor reducing power of ascorbate (*vide supra)*. Six samples of the nitrosylated mouse liver lysates [5 mg/mL, 75 μL] were subjected to the three step TST protocol: (1) blocking with SPSC (16 nmol in pH 4.0 buffer, 1 h, dark, ambient temperature), (2) conversion to *S*-phenylsulfonylcysteine residues with $PhSO_2Na$ (2.5 mmol in pH 4.0 buffer, 30 min, dark, ambient temperature) and (3) labeled with the three Z-Cy-SH probes [Z-Cy2-SH, Z-Cy3-SH and Z-Cy5-SH (each 0.8 nmol in DMF, 10 min, dark, ambient temp)]. Each dye (Z-Cy2-SH, Z-Cy3-SH and Z-Cy5-SH) was used to label two samples each (a GSNO sample and a UV knockout negative control.) Excess Z-Cy-SH dye was quenched with the addition of 80 nmol MMTS and samples were run on 1D non-reducing SDS-PAGE gels. Early experiments were focused on optimization of the blocker to dye ratio in order to maximize labeling while preventing background or false labeling of free thiol. As in the experiment above, this ratio was determined to be 20:1 blocker to dye. After fluorescence images were obtained using each of the three Typhoon light filters, the gel was stained overnight with coomassie blue and destained for 1 hour to show total protein content for each lane.

It is clear from the fluorescence images (**Fig. 17**) that background labeling (shown in the right lanes) is reduced in comparison to fluorescent SNO-labeled proteins (left lanes), given roughly equivalent amounts of protein loaded.

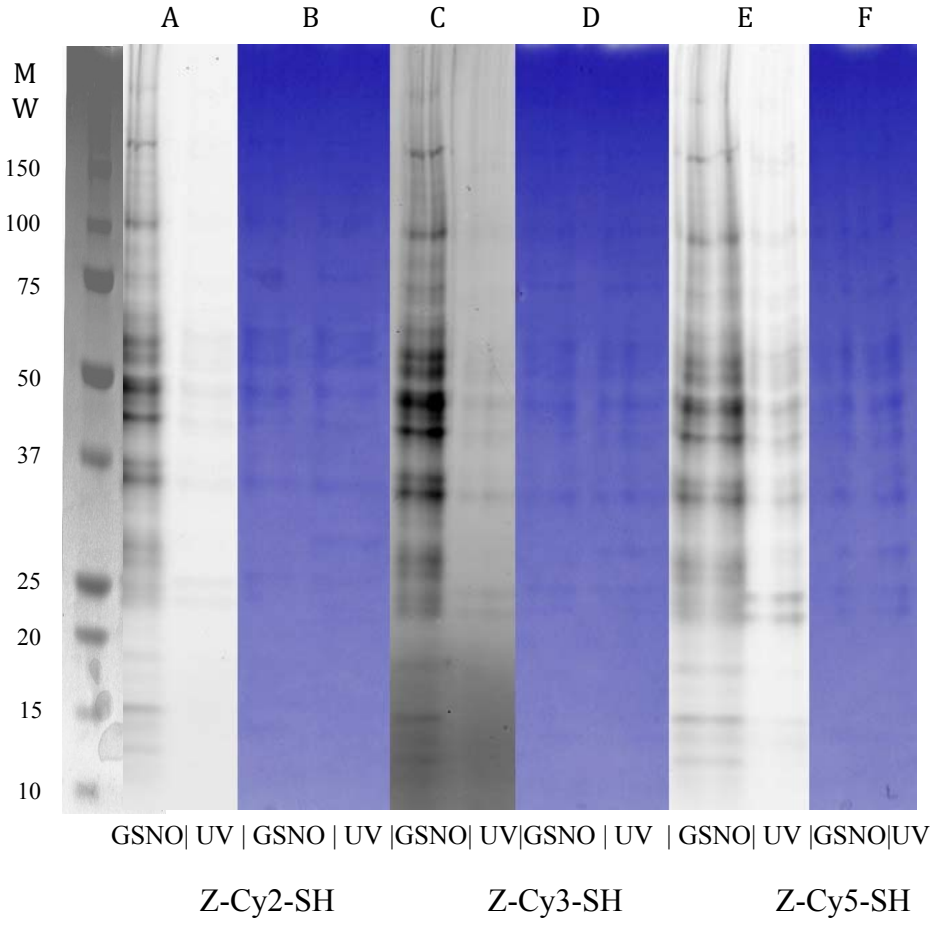

Figure 17. Fluorescent images of SNO labeled mouse liver lysate (left lanes) and UV knockout negative control (right lanes) using Z-Cy2-SH (A), Z-Cy3-SH (C) and Z-Cy5-SH (E), with accompanying coomassie staining of A, C and E shown with B, D and F respectively.

The Modified Biotin Switch Technique Protocol

Prior to demonstrating the ability of the TST to label SNO, a modified BST protocol was developed to run head-to-head with the TST. This protocol employed the standard blocking and reduction steps of the BST (blocking with 5 µL MMTS in 2.5% SDS, pH 8.0 HEN buffer, 37 °C, for 20 min followed by acetone precipitation and resuspension in pH 8.0 HENS (HEN buffer with 1% SDS (w/v)) buffer with 80 mM ascorbate), but employs an electrophilic OPSS (**Fig. 18**) or maleimide (**Fig. 19**) Z-CyDye to label. The Z-Cy-OPSS and Biotin-HPDP (**Fig. 6**) bear the same thiol reactive chain, so the thiol reactivity of the Z-CyDye fluorescent probe in the modified biotin switch protocol is the same as that of the Biotin-HPDP in the classical biotin switch technique.

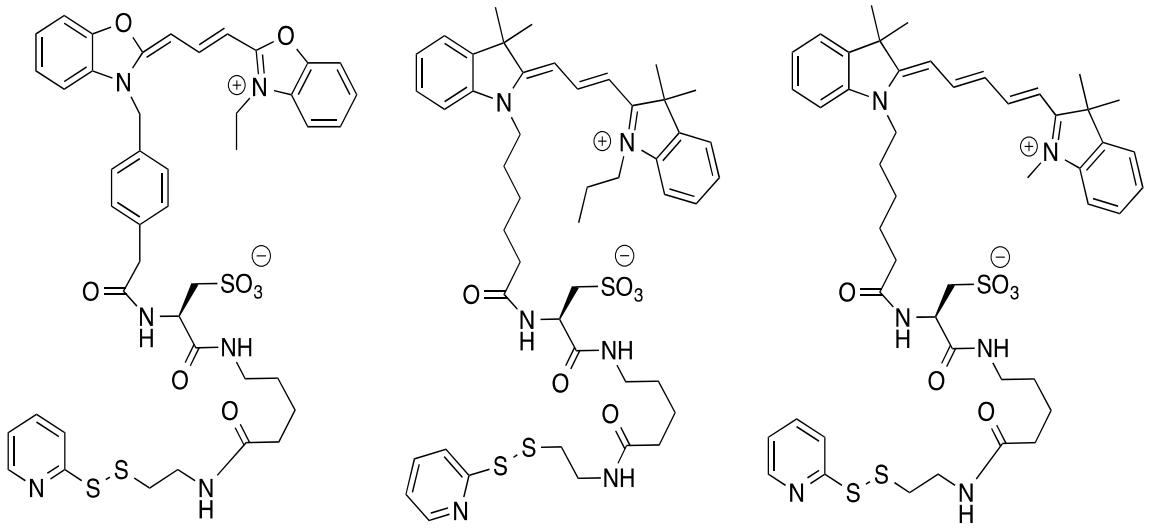

Figure 18. Structures, from right to left, of Z-CyDye OPSSs Z-Cy2-OPSS, Z-Cy3-OPSS and Z-Cy5-OPSS

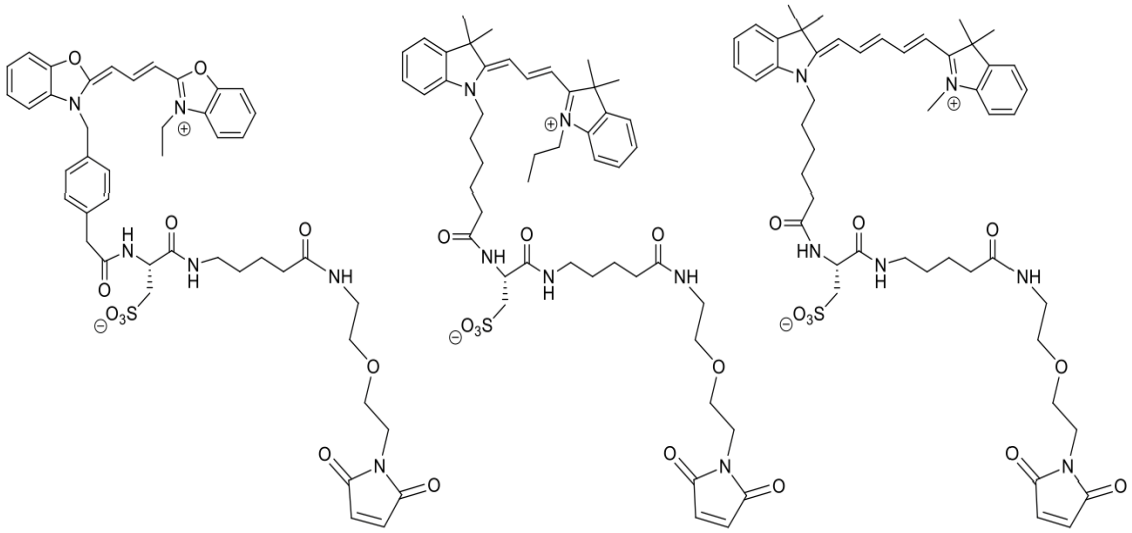

Figure 19. Structures, from left to right, of Z-CyDye Maleimide Z-Cy2-Mal, Z-Cy3-Mal and Z-Cy5-Mal

In order to confirm the efficacy of the modified BST, two samples of mouse liver lysate (75 µL, 5mg/mL protein) were nitrosylated (200 nmol GSNO in pH 8.0 HEN buffer for 200 µg protein, 1 h, dark, ambient temperature). One of the two samples was subjected to an ascorbate knockout control (80 mM for 1 h in the dark at ambient temperature) and both were spun over Microbiospin 6 columns preequilibrated to pH 8.0. Both samples were labeled by the modified BST: (1) blocking (5 µL MMTS in 2.5% SDS, pH 8.0 HEN buffer, 37 °C, for 20 min followed by acetone precipitation and resuspension in pH 8.0 HENS buffer), (2) reduction and labeling (80 mM ascorbate, 8 nmol Z-Cy-OPSS for 1 h in the dark at ambient temperature). The SNO sample was labeled with Z-Cy5-OPSS and the ascorbate knockout control with the Z-Cy3-OPSS. The samples were combined (67 µL each, 35 µg protein each) with IEF buffer (7 M urea, 2 M thiourea, 4% CHAPS, 2 µL IPG NL 3-11ampholytes) to give a total volume of 450 µL which was focused on Immobulin Drystrips NL 3-11 and run on 2D non-reducing SDS-

PAGE 14% acrylamide gels at a constant wattage of 2W/gel. The gel was scanned immediately after it had finished focusing on the GE Typhoon Trio scanner at excitation/emission wavelengths (nm) of 532/580 (Cy3) and 633/670 (Cy5) with photomultiplier tube voltage at 600V and 100 micron resolution.

The gels clearly show the labeling of specific proteins. Moreover, the Z-Cy5-OPSS labeled gel image (SNO labeled, **Fig. 20**) has more intense labeling than the Z-Cy3-OPSS labeled gel image (ascorbate knockout, **Fig. 21**.) However, the visible presence of labeled proteins in the ascorbate knockout sample again indicates that ascorbate is not reducing all SNO present in the sample. The streaking and poor resolution of this gel most likely stems from focusing issues associated with pH solubility of proteins. However, these gels clearly show the ability of the modified BST to label SNO selectively.

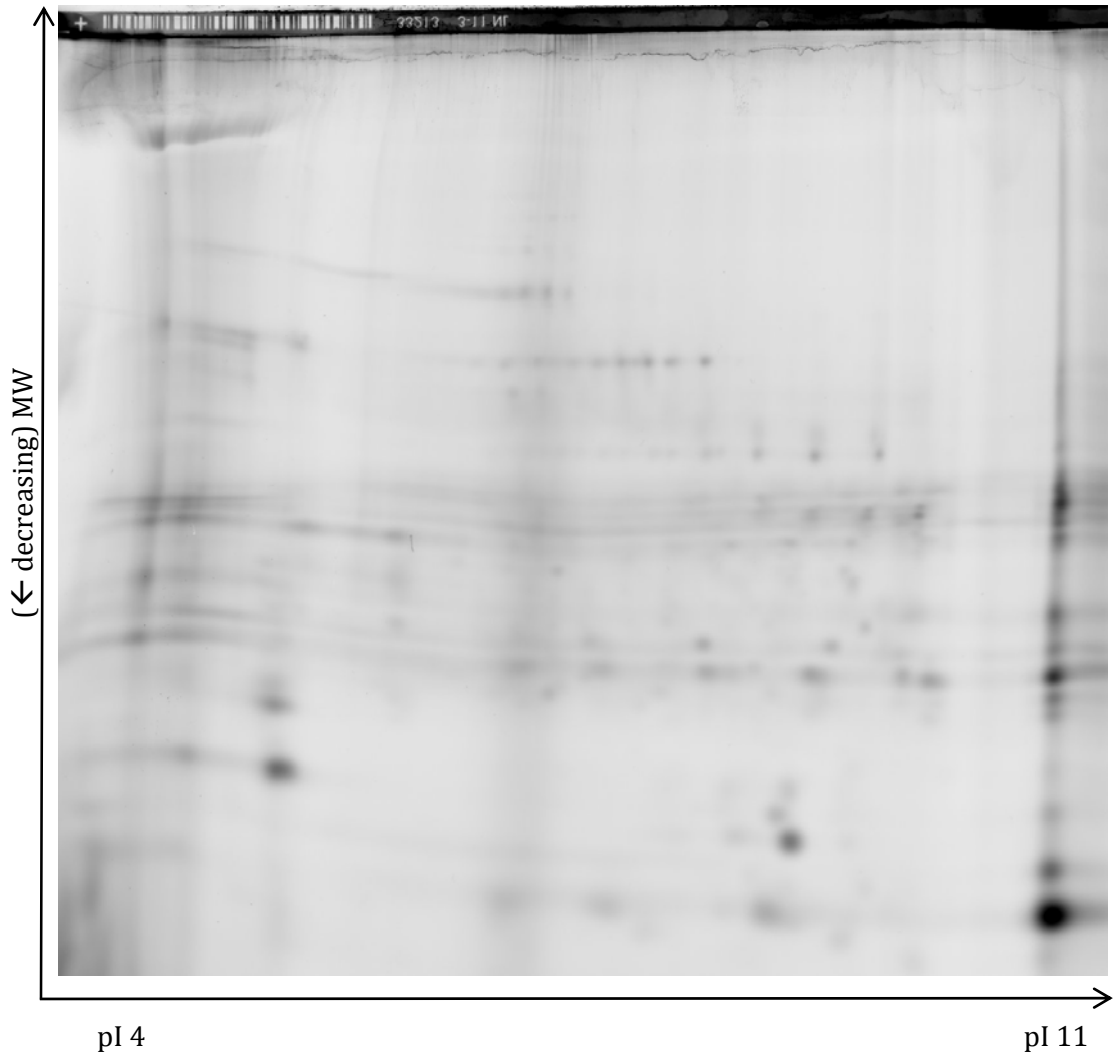

Figure 20. Fluorescence 2D gel image of BST labeled mouse liver lysate, nitrosylated with GSNO and labeled with Z-Cy5-OPSS.

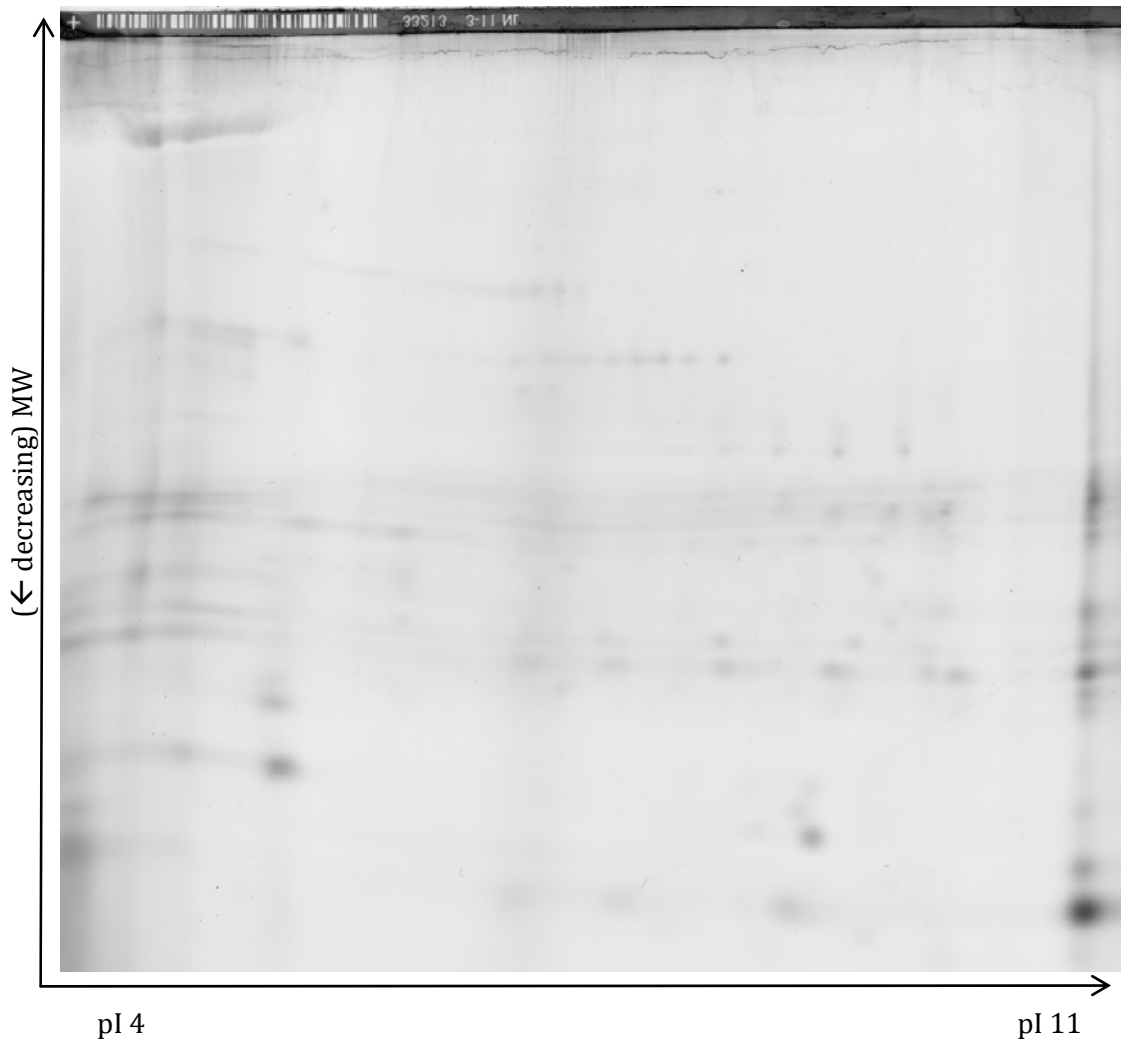

Figure 21. Fluorescence 2D gel image of BST labeled mouse liver lysate, nitrosylated with GSNO, subjected to ascorbate knockout control and labeled with Z-Cy3-OPSS.

TST vs Modified BST: Comparitive 1D and 2D Gel Analysis

To directly compare the abilities of the TST and BST to label S-nitrosothiols, the protocols were performed side-by-side on equivalent amounts of protien (confirmed by both coomassie staining and a Bradford concentration assay (BCA). Samples of mouse

liver lysate (75 mg/mL, 5 µL in 50 µL pH 8.0 HEN buffer) were *S*-nitrosylated employing GSNO (20 µL, 10 mM in pH 8.0 HEN buffer for 1h in the dark at ambient temperature) and were subsequently spun over Biorad Microbiospin 6 columns, equilibrated with either pH 4.0 ammonium formate or pH 8.0 HEN buffer.

The thiosulfonate switch protocol was carried out on the liver lysis samples, buffer exchanged to pH 4.0, and the modified BST on liver lysate samples exchanged to pH 8.0. UV knockout controls were performed after samples were spun over the columns. For endogenous samples, 20 µL of pH 8.0 HEN buffer was substituted in place of the GSNO. TST samples were labeled using the standard protocol, employing 20µL of 10 mM SPSC to block free thiols and labeled with 8 nmol of Z-Cy3-SH. The BST samples were also labeled using the standard conditions and labeled with 8 nmol of Z-Cy3-Mal. After scanning, the gel was stained with coomassie blue for 4 h and destained for 1 h. The increased spot volume of the SNO-labeled TST and the decreased background labeling in comparison to the BST samples, shown in **Fig. 22**, demonstrates that the thiosulfonate switch has greater sensitivity and fewer false positives in comparison to the biotin switch assay. Both samples show almost universal labeling of proteins by the fluorescent probes, indicating that most proteins of the lysate were nitrosylated.

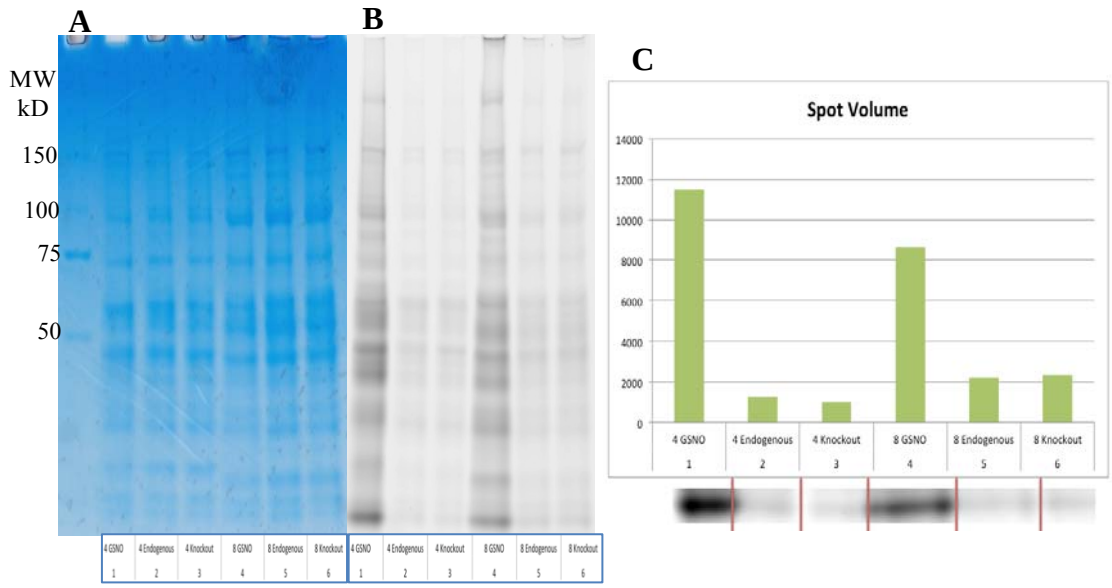

Figure 22. (A) Scanned image of labeled gel after coomassie staining showing roughly equivalent amounts of protein. (B) Fluorescent images of nitrosylated mouse liver labeled by the TST (4) and the modified BST (8) with endogenous and UV knockout controls. (C) Spot volumes, obtained from ImageJ software, showing spot intensity of a single spot labeled by both protocols.

Many of the problems associated with the biotin switch assay are derived from its use of ascrobate as a reducing agent. Ascorbate is an inefficient reductant for pure protein *S*-nitrosothiols. To compare the ability of ascorbate to reduce SNO proteins in lysates, eight mouse liver lysate samples (55 µL, 375 µg total protein) were nitrosylated by GSNO (20 µL, 10 mM in pH 8.0 HEN buffer for 1h in the dark at ambient temperature), followed by purification on microbiospin 6 columns to remove excess GSNO. Four samples were spun over pH 4.0 preequilibrated microbiospin 6 columns and four samples over pH 8 preequilibrated microbiospin 6 columns. Two pH 4.0 liver lysate samples and two pH 8.0 liver lysate samples were chosen as SNO knockouts and one of each sample (one pH 4.0 and one pH 8.0 sample) was irradiated at 312nm UV light for 10 min while the other was mixed with ascorbate (final concentraion of 10 mM) for 30 min in the dark

at ambient temperature in an attempt to reduce all SNO present. Ascorbate samples were subsequently spun over microbiospin 6 columns, one sample to pH 4 and the other to pH 8, to remove any residual ascorbate and both UV and ascorbate samples were carried through the TST (pH 4) or BST (pH 8) as described previously.

In previous experiments, free glutathione (GSH) had been removed from the samples by the microbiospin 6 columns, so labeling experiments had not been conducted in the presence of physiological concentrations of glutathione. As glutathione is one of the cell's most important thiol signaling messengers, its presence could potentially interfere with the two protocols. After samples were nitrosylated by GSNO and purified by microbiospin columns, the pH 4 and the pH 8 samples each received GSH to a final concentraion of 5mM.

The heavy labeling (**Fig. 23**) of the ascorbate knockout samples, both using the TST and BST protocols, indicates that SNO has not been fully reduced. This result is yet another example of ascorbate's poor reduction potential with regards to *S*-nitrosothiols at ambient conditions and thus carries more implications about the inability of the BST to label all SNO moieties. Also, for both the TST and BST samples, the presence of physiological concentrations of GSH interupts labeling. This result must be adressed further employing *in-vivo* studies on cell lines or intact tissue.

Previously, the labeling of a BSA/BSA-SNO mixture with varying amounts of SNO had been performed (**Fig. 12**) to assess the TST's ability to label only *S*-nitrosylated proteins. This experiment was repeated for mouse liver lysates by varying the amount of GSNO initially added to the sample. To eight samples of mouse liver

lysate (75 µL, 5 mg/mL each, pH 8.0 HEN buffer) was added GSNO (1h, dark, ambient temperature) using the following concentartions of GSNO: 1 mM, 10 µM, 0.1 µM and 10 nM. One sample of each GSNO concentration was spun over a pH 4 preequilibrated microbiospin 6 column providing samples to be analyzed by the TST protocol, while the other four were spun over pH 8.0 preequilibrated columns for analysis by the BST protocol. The pH 4 (TST) samples were blocked with SPSC (16 nmol, 1 h, dark, ambient

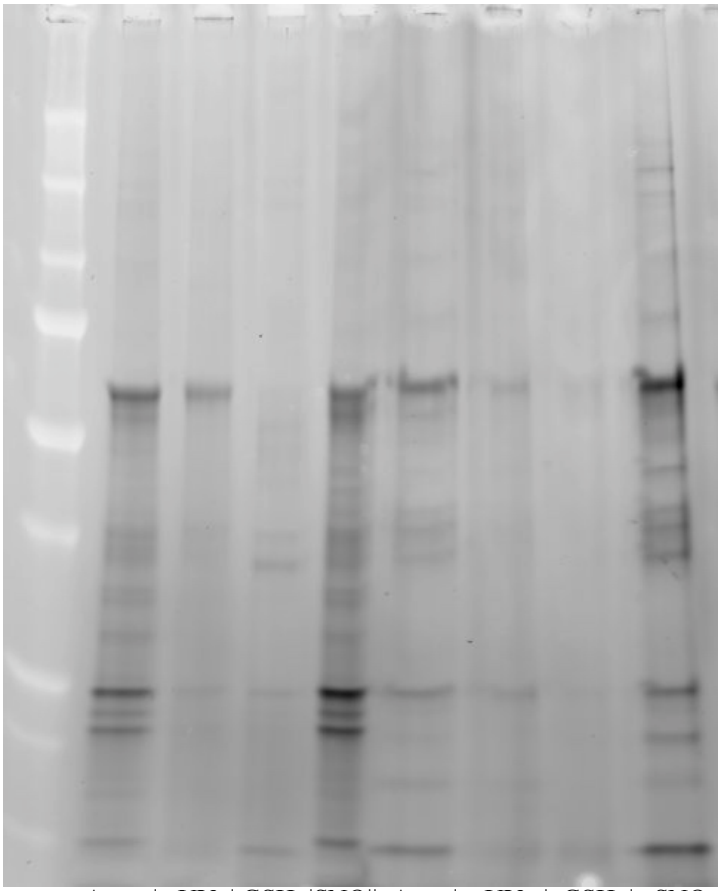

Figure 23. Fluorescence image of TST and BST labeled mouse liver lysate with ascorbate and UV SNO knockouts and GSH doped samples with standard GSNO nitrosylated positive control.

temperatrue), converted to *S*-phenylsulfonylcysteine residues with $PhSO_2Na$ (2.5 mmol, 30 min, dark, ambient temperature) and labeled with Z-Cy3-SH (4 nmol in DMF, 10 min, dark, ambient temperature). Excess Z-Cy3-SH dye was quenched by the addition of 80 nmol of MMTS and samples were run on 1D SDS-PAGE non-reducing gels. The fluorescence gel image, **Fig. 24A**, shows almost universal labeling of proteins in the lysate for the TST lanes (lanes 1-4) and the BST lane with the highest amount of GSNO added (lane 5); however, the remaining BST lanes (6-8) show only a few protein spots and the spot intensity changes very little despite gradual decrease in nitrosant concentraion. Two protein spots labeled with the TST, visible in each of the four lanes, have been labeled as TST spot 1 and TST spot 2. Two other protein spots labeled with the BST, also visible in all four BST lanes, have been labeled as BST spot 1 and BST spot 2. The spot volumes of each protein in each gel were measured by ImageJ and the spot volume was plotted against the amount of nitrosant added. The two BST spots show very little change in spot volume despite 10 to 100 fold change in nitrosant added. This is in stark contrast to the TST spots that show a linear response of [GSNO] vs spot volume as shown in **Fig. 24B**. The poor linearity of the modified BST's spot volumes vs the amount of GSNO present may indicate that available NO is being taken up by a select few proteins that are in turn more heavily labeled or that any available NO is immediately transferred from its initial protein *S*-nitrosothiol to the heavily labeled proteins (transnitrosation). It is clear, however, that at lowered [GSNO], the TST protocol labels more proteins than the modified BST protocol.

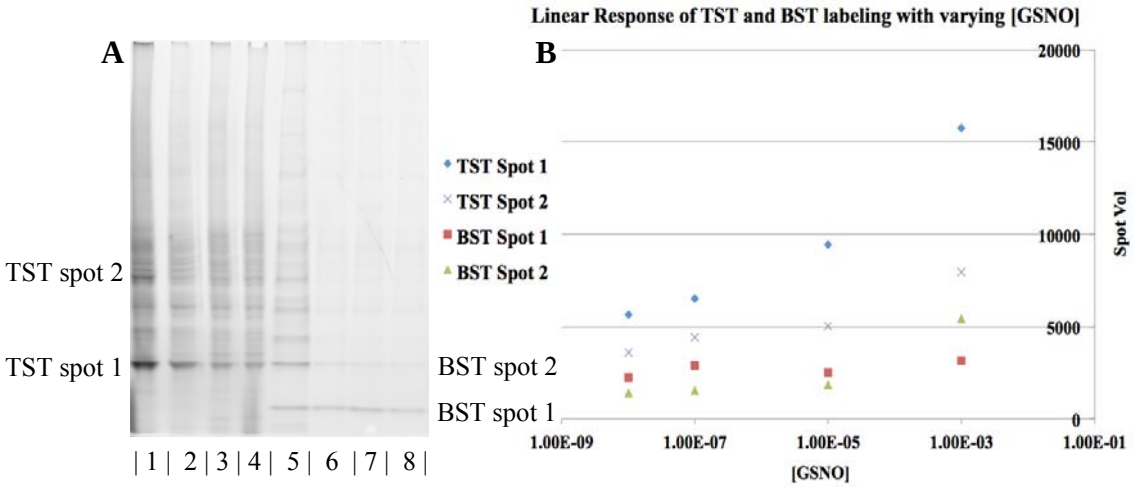

Figure 24. (A) Fluorescence image of 1D non-reducing SDS-PAGE gel with varying amounts of GSNO (decreasing [GSNO] from left to right). Lanes 1-4 are the TST labeled mouse liver lysate and lanes 5-8 are the BST labeled mouse liver lysate. Concentration of added GSNO decreases from left to right. (B) Plot of spot volume vs final [GSNO].

To continue to assess the scope and limitations of the TST, labeled samples run on 2D gels to give a more defined overall picture of the labeling of the lysate. To this end, two mouse liver lysate samples (55 µL, 375 µg total protein each) were nitrosylated by GSNO (20 µL, 10 mM in pH 8.0 HEN buffer for 1h, dark, room temperature) and purified by microbiospin 6 columns with buffer exchanged to pH 4.0 or pH 8.0 to remove excess GSNO. To generate a negative SNO knockout control, the pH 8 sample was combined with ascorbate (50 mM, 1 h, dark, ambient temperature) and was purified by microbiospin 6 columns preequilibrated to pH 4.0. Both samples were carried through the TST protocol as described earlier: 1) SPSC (16 nmol, 1 h, dark, ambient temperature), 2) $PhSO_2Na$ (2.5 µmol, 30 min, dark, ambient temperature), 3) Z-Cy3-SH (ascorbate KO sample) or Z-Cy5-SH (GSNO sample) (0.8 nmol in DMF, 10 min, dark, ambient

temperature), 4) MMTS (80 nmol.) The samples were combined with a Z-Cy2-SH labeled internal standard, derived from mixing equal portions of the two samples before labeling with either Z-Cy3-SH or Z-Cy5-SH. The Z-Cy2-SH sample was also labeled with 0.8 nmol for 10 min in the dark at ambient temperature and quenched with 80 nmol of MMTS. The combined samples (67 μL, 150 μg total protein) were diluted to a final volume of 450 mL with IEF buffer and focused on Immobulin Drystrips NL 3-11 using the standard focusing procedure. After focusing, the strips were run on 14% accrylamide 2D gels at a constant wattage of 2W/gel. Fluorescence images were obtained at all three excitation wavelengths for the three Z-CyDyes.

It is clear from the 2D gel images that the GSNO sample (**Fig. 25**) exhibits much stronger labeling than the ascorbate SNO knockout control sample (**Fig. 26**.) The Z-Cy2-SH labeled standard (**Fig. 27**) shows an intermediate amount of labeling compared to the GSNO and KO samples. However, there is still a significant amount of labeling in the ascorbate knockout sample. This experiment was repeated with a 5 min UV knockout instead of the ascorbate KO. The TST labeled GSNO sample (**Fig. 28**) shows clear labeling of SNO proteins as expected, however, the UV knockout (**Fig. 29**) shows almost no labeling. It is clear that the ascorbate knockout sample has much higher labeling levels than the UV knockout. This is another example of ascorbate's inability to reduce all SNO present in a lysate. The Z-Cy2-SH standard with the UV knockout (**Fig. 30**) shows an intermediate amount of labeling, as expected.

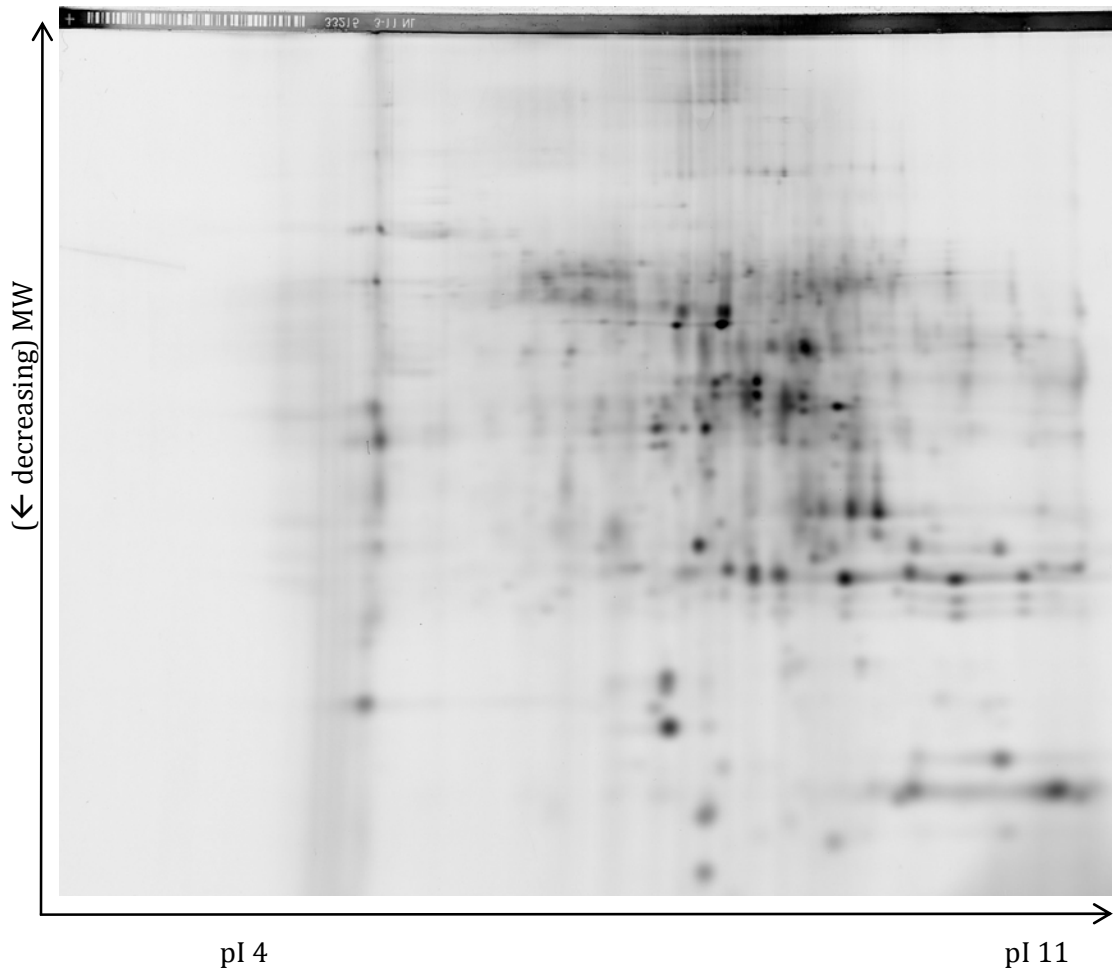

Figure 25. Fluorescence 2D gel image of TST labeled mouse liver lysate, nitrosylated with GSNO and labeled with Z-Cy5-SH.

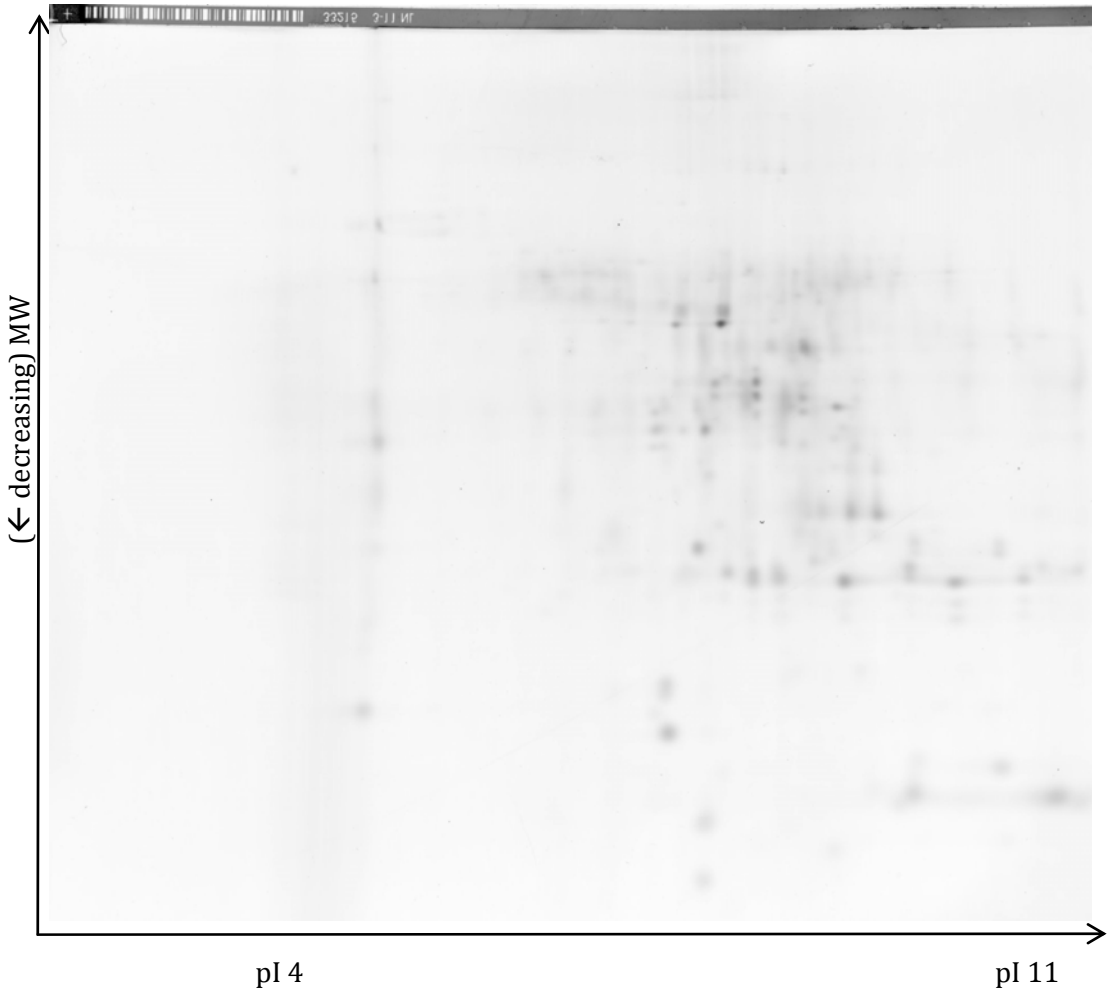

Figure 26. Fluorescence 2D gel image of TST labeled mouse liver lysate, nitrosylated with GSNO, subjected to ascorbate knockout control and labeled with Z-Cy3-SH.

The thiosulfonate switch technique protocol has been applied to numerous protein samples of varying complexity and has shown to be an accurate, fast and non-disruptive technique with respect to thiol redox state. The TST had previously been performed on small molecules (GSNO), single pure *S*-nitrosylated proteins (BSA-SNO), and two pure protein mixtures (BSA-SNO/AdhR*-SH and BSA/AdhR*-SNO) and clearly show labeling of *S*-nirosothiols with fluorescent Z-Dyes (Rhod-SH and Z-Cy-SH probes). The

TST has also shown negligible levels of labeling of free thiol with the inclusion of SPSC as a thiol blocker. To further assess the scope and limitations of this technique, the TST has been applied to mouse liver lysates.

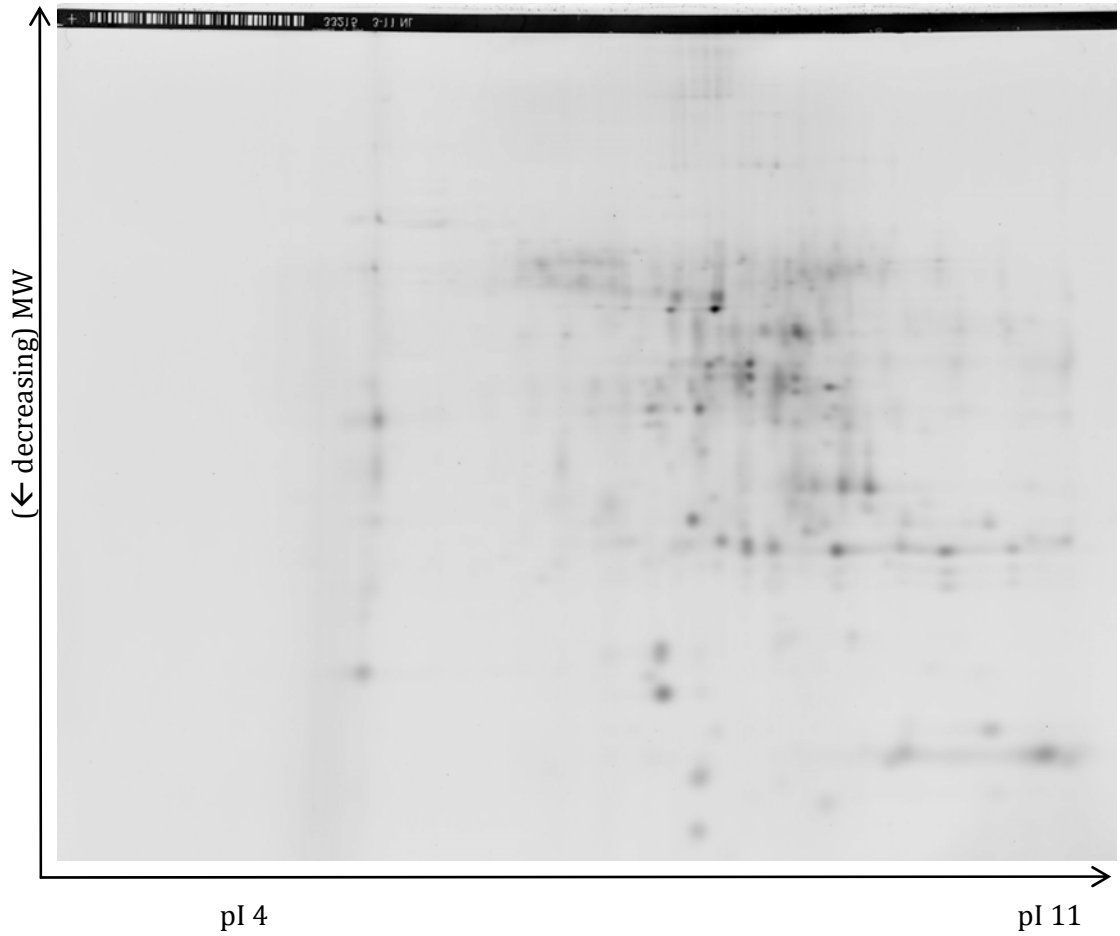

Figure 27. Fluorescence 2D gel image of TST labeled mouse liver lysate with ascorbate knockout Z-Cy2-SH labeled internal standard.

The 1D and 2D gel images presented indicate that the TST protocol is successfully labeling SNO proteins with minimal labeling of knockout (no SNO present) samples. The use of the modified BST, developed in the Grieco laboratory, also exhibits labeling selectivity for *S*-nitrosothiols. Furthermore, the TST has shown higher labeling

efficiency (greater spot volume) and less background labeling in comparison to the modified BST technique in 1D and 2D gel studies.

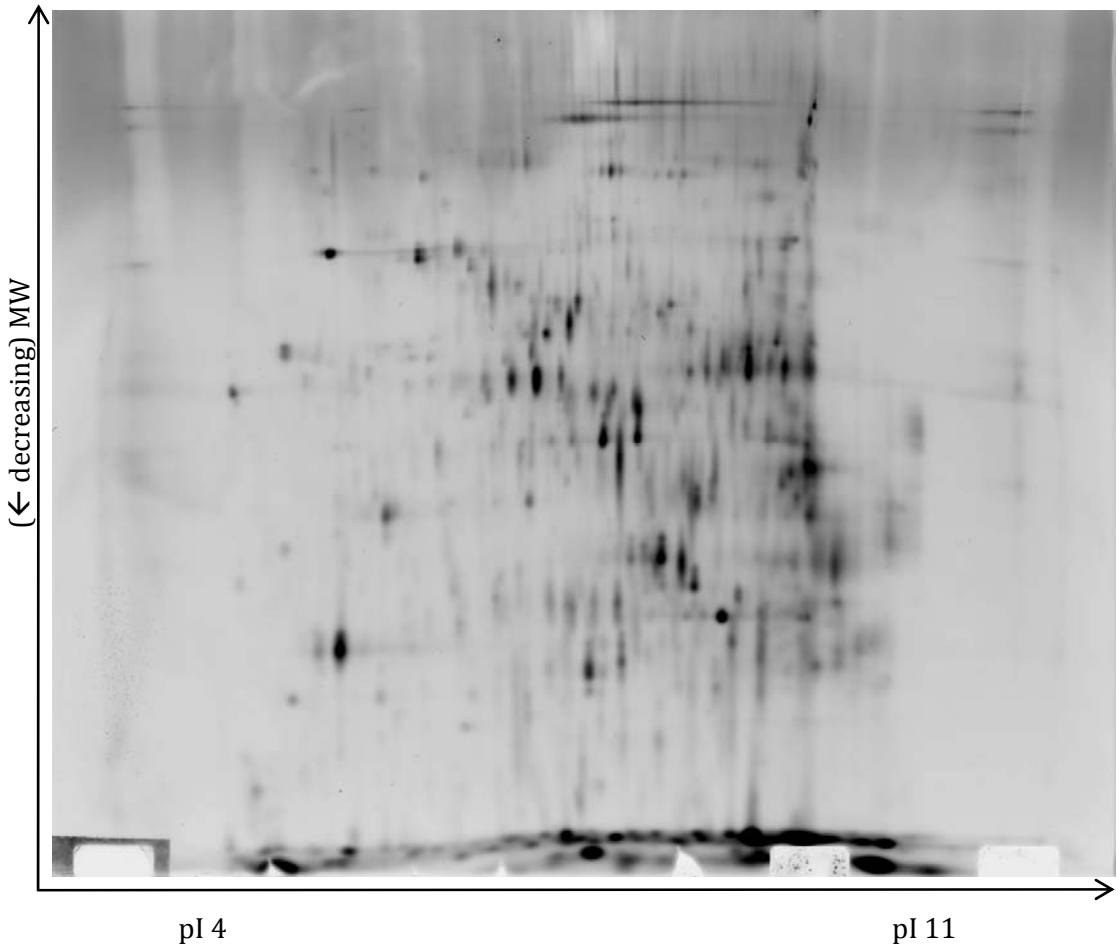

Figure 28. Fluorescence 2D gel image of TST labeled mouse liver lysate, nitrosylated with GSNO, and labeled with Z-Cy3-SH.

This work clearly demonstrates the ability of the TST to be applied to lysate protein samples. Further work on the TST will be directed towards inclusion of this protocol in the analysis of *S*-nitrosothiols of whole cells or cell lines as well as the TST's adaptation for more high-throughput mass spectrometry applications.

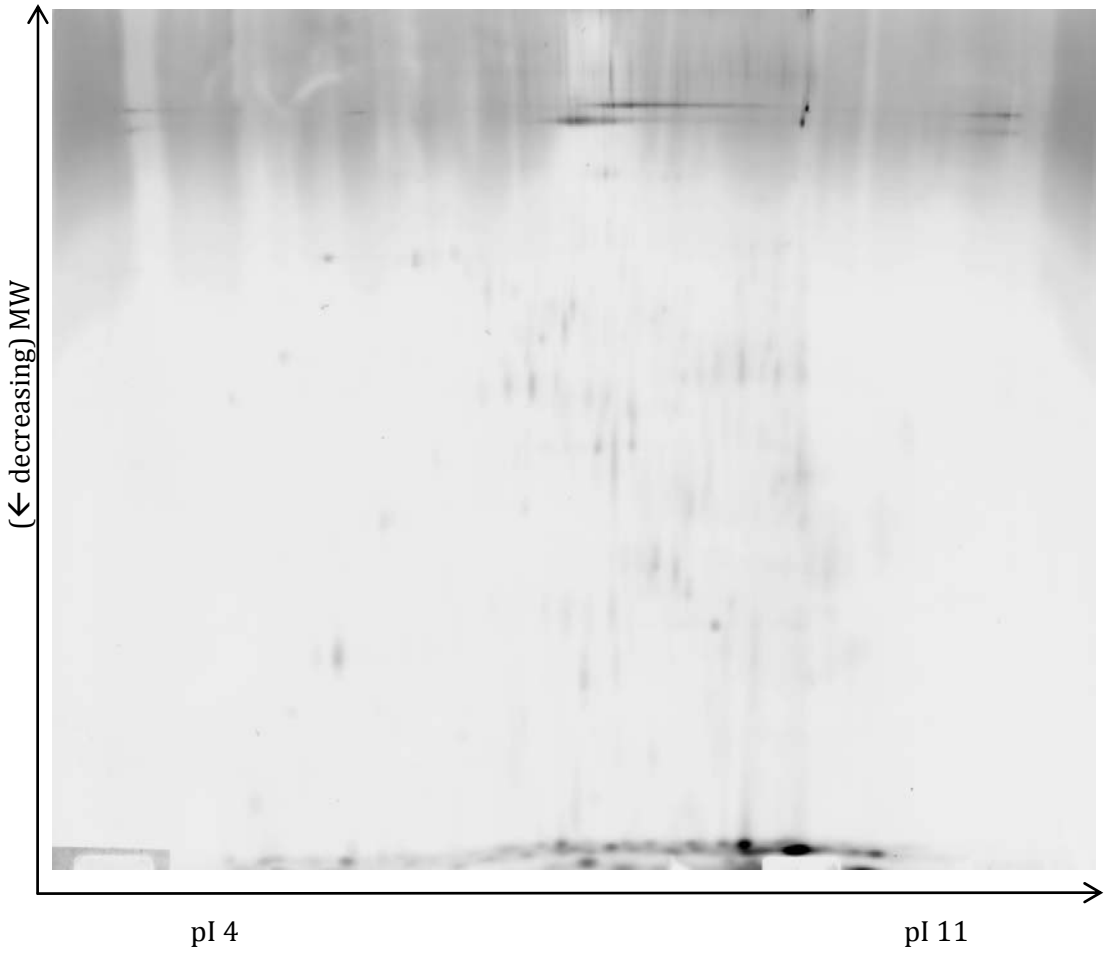

Figure 29. Fluorescence 2D gel image of TST labeled mouse liver lysate, nitrosylated with GSNO, subjected to a 5 min UV knockout control and

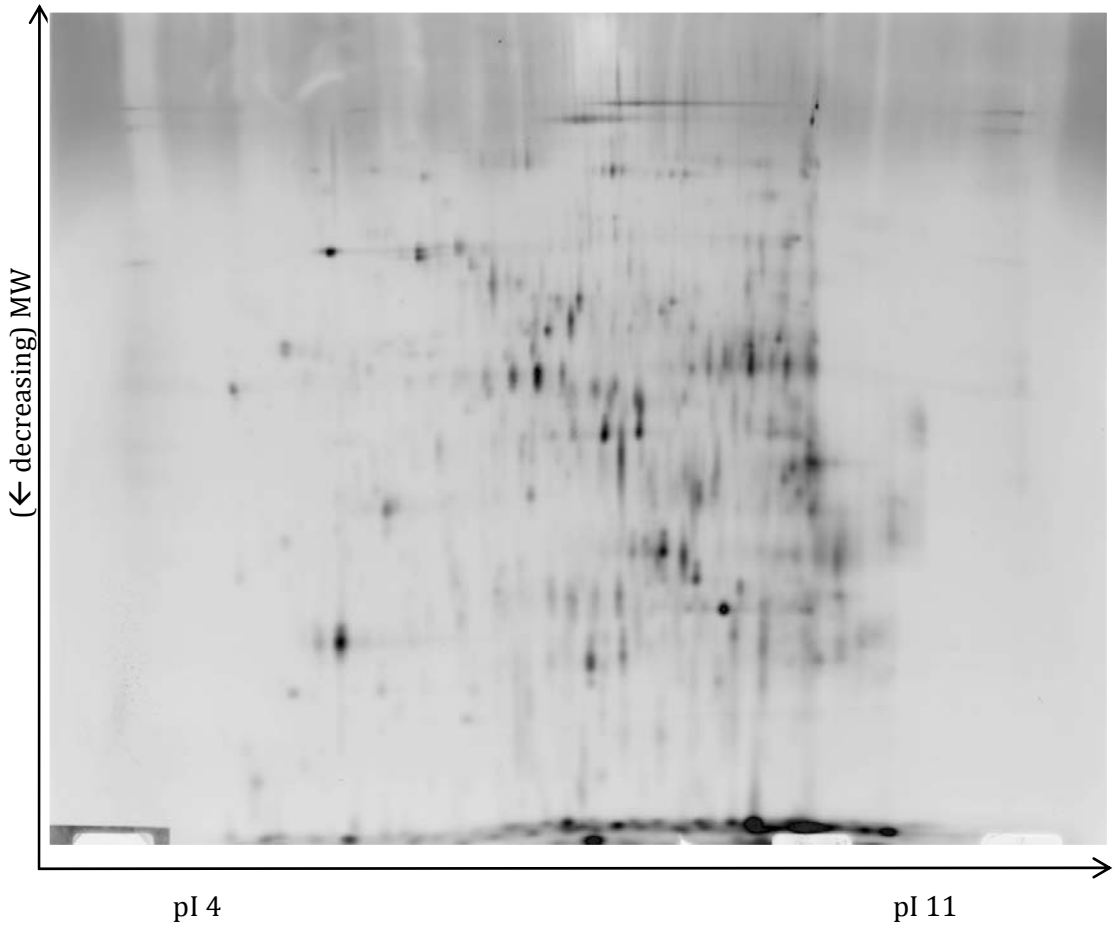

Figure 30. Fluorescence 2D gel image of TST labeled mouse liver lysate with 5 min UV knockout Z-Cy2-SH labeled internal standard.

SYNTHETIC EFFORTS

Synthesis of SO_3-Cy-Mal 2nd Generation Z-CyDyes

The efficiency of the Z-Cydyes has been well established both through this work and previously published work.[27] Z-Cydyes, however, can be synthetically challenging, especially in regards to the installation of the cysteic acid motif which is employed to increase solubility match isoelectric points (PI). Therefore, a Zdye with similar zwitterionic character but more easily and readily synthesized became an important target. To avoid the use of linker chain bearing a cysteic acid moiety, a cyanine dye with a sulfonic acid residue on the aromatic portion of the cyanine core was investigated. The first Z-Cydye possessing a sulfonic acid residue on a cyanine fluorophore was synthesized by Mark Epstein in the Grieco Laboratory; the sulfonic acid derivative of the Cy5 maleimide (SO_3-Cy5-Mal) (**Fig. 31**) was successfully synthesized and required fewer steps to complete. While the Cy2 dye of this family was unable to be produced, the Cy3 derivative was also successfully synthesized. Thus, a two color, zwitterionic cyanine dye set had been successfully synthesized, thus eliminating the cysteic acid moiety in the linker side chain.

(SO3-Cy3-Mal) The synthesis of the zwitterionic Cy3 maleimide bearing a sulfonic acid residue began with the condensation of 3-methyl-2-butanone with 4-hydrazinobenzenesulfonic acid to give the sulfonic acid indole **I**, which was deprotonated with KOH in methanol and n-propanol to give sulfonate indole **II**. Alkylation of **II** with 6-bromohexanoic acid in 1,2-dichlorobenzene and tetrabutylammonium iodide gave the

indolium salt **III**, which was condensed with the previously synthesized (*E*)-*N*-(2-(3,3-dimethyl-3H-indol-2-yl)vinyl)-*N*-phenylacetamide to give the carboxylate cyanine chromophore **IV**. The free acid was activated with *N*-hydroxysuccimide in the presence of *N*-diisopropylcarbodiimide and DMF to give the NHS ester **V**. The maleimide dye **VI** was realized by reaction of the NHS **V** ester with *N*-(2-Aminoethyl)maleimide in DMF containing *N*-methylmorpholine (**Fig. 32**).

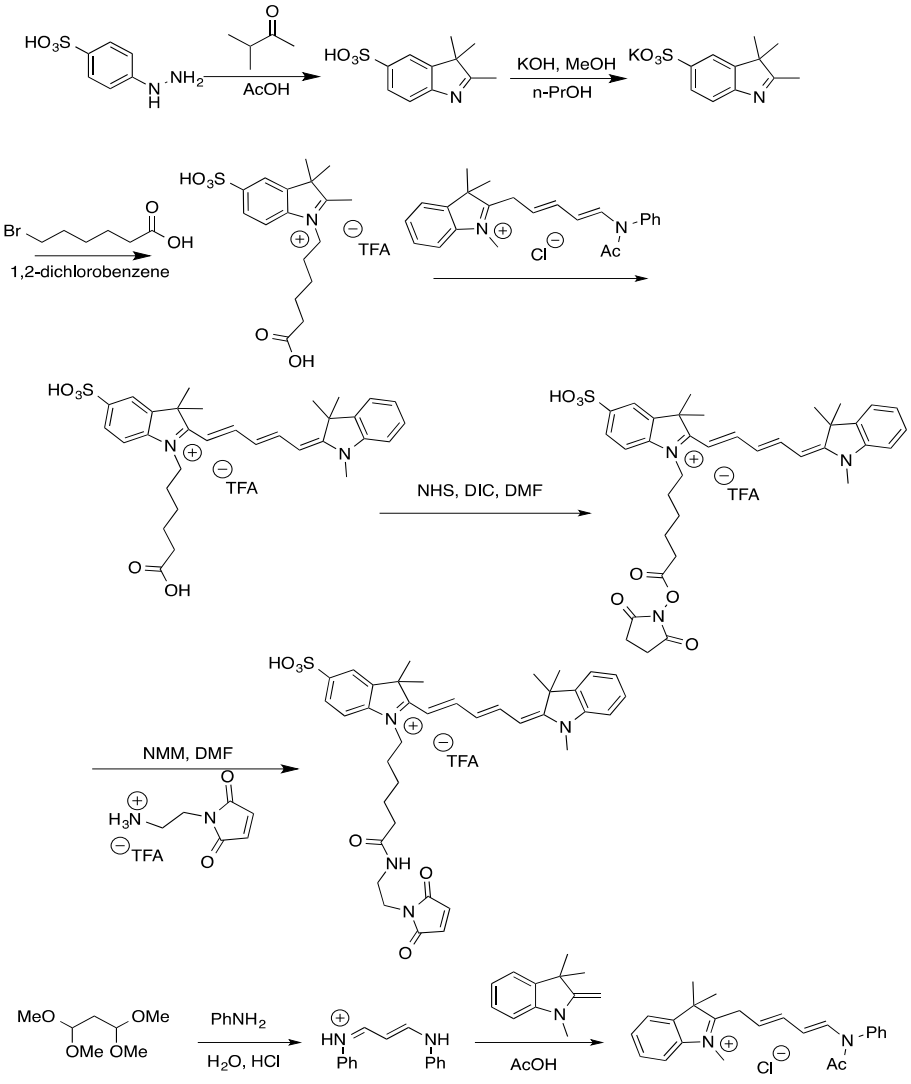

Figure 31. Synthetic route for the sulfonic acid Cy5 maleimide (SO_3-Cy5-Mal)

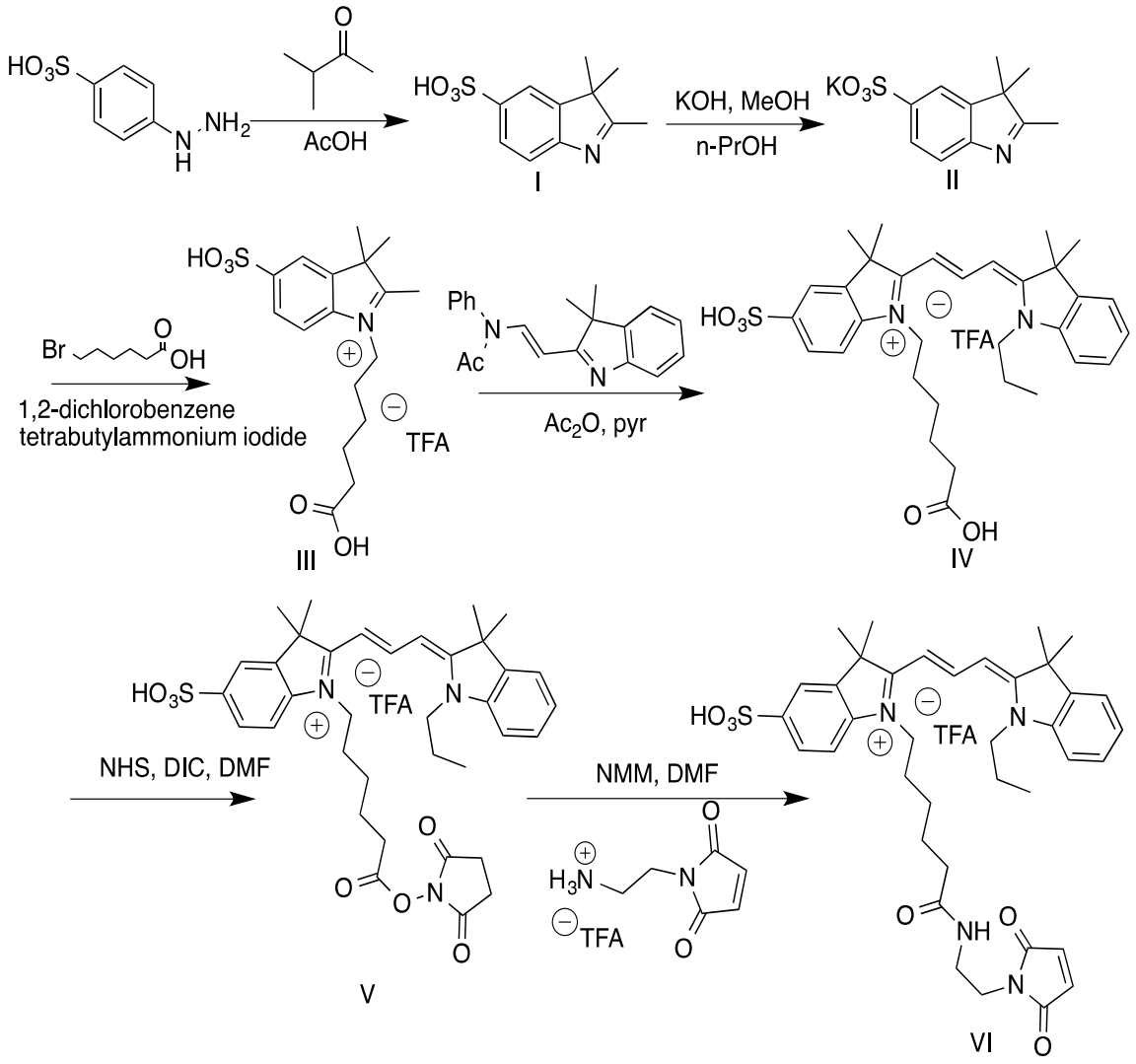

Figure 32. Synthetic route for the sulfonic acid Cy3 maleimide dye (SO_3-Cy3-Mal)

Comparison of 1st and 2nd Generation
Z-Cy-Mal Dyes by 2D-DIGE Analysis

The completion of the synthesis of the SO_3-Cy-Mal dye set proved that a more efficient route to a zwitterionic cyanine dye could be achieved. However, the ability of these dyes to label proteins had not yet been established. To this end, the saturation thiol

labeling of mouse liver lysate was conducted using DIGE with SO_3-Cy3-Mal/Z-Cy5-Mal and SO_3-Cy5-Mal/Z-Cy3-Mal dyes.

The mouse liver lysates (75 mg/mL, 5 μL, in 370 μL saturation labeling buffer, pH 8.0) were aliquoted into 20 μL fractions of 1 mg/mL concentration, labeled with 4 nmol of maleimide dye for 30 min at 37 °C in the dark. The reactions were quenched by the addition of 150 μL of stopping buffer (7 M urea, 2 M thiourea, 4% CHAPS, 0.5% IPG ampholytes, 0.01% bromopehnyl blue). An isoelectric focusing sample was prepared by adding 67 μL of the SO_3-Cy3-Mal labeled sample with 67 μL of the Z-Cy5-Mal labeled sample and 320 μL IEF buffer to give a final volume of 450 μL. Another sample was prepared by adding 67 μL of the SO_3-Cy5-Mal and 67 μL of the Z-Cy3-Mal labeled solutions with 320 μL of IEF buffer. Each IEF sample was focused on NL 3-11 Immobulin Drystrips using the Ettan IPGphor2 IEF system and the standard voltage steps (detailed in experimental). Focused proteins were separated on 14% acrylamide SDS-PAGE non-reducing gels with a constant wattage of 2W/gel.

In comparing the SO_3-Cy3-Mal (**Fig. 33**) and Z-Cy5-Mal (**Fig. 34**) thiol labeling gels, both exhibit roughly equivalent labeling levels. Furthermore, the total number of spots and their locations is also almost identical. The location on the gel of labeled protein spots is most almost identical between first and second generation. The highlighted areas of the gel (yellow lin, blue and red circles) are areas of high protein labeling that are easily distinguished in both gels for comparison of the labeling potential. This supports the original hypothesis that a sulfonic acid derivative of the original

cyanine dyes labels proteins with similar efficiency as the Z-CyDye probes, yet requires fewer steps and offers higher yields of the respective dyes.

It is clear from the gels that the second generation SO_3-Cy-Mal probes act with similar reactivity as the first generation Z-Cy-Mal set and that their labeling intensities are roughly equivalent. The replacement of the cysteic acid in the linker side chain with a sulphonate residue on the aromatic ring of the flourophore does not change the labeling ability of the 2^{nd} generation (SO_3-Cy-Mal) as evidenced by the similarity of the two gels in terms of spot location, spot intensity and presence of background (false) labeling.

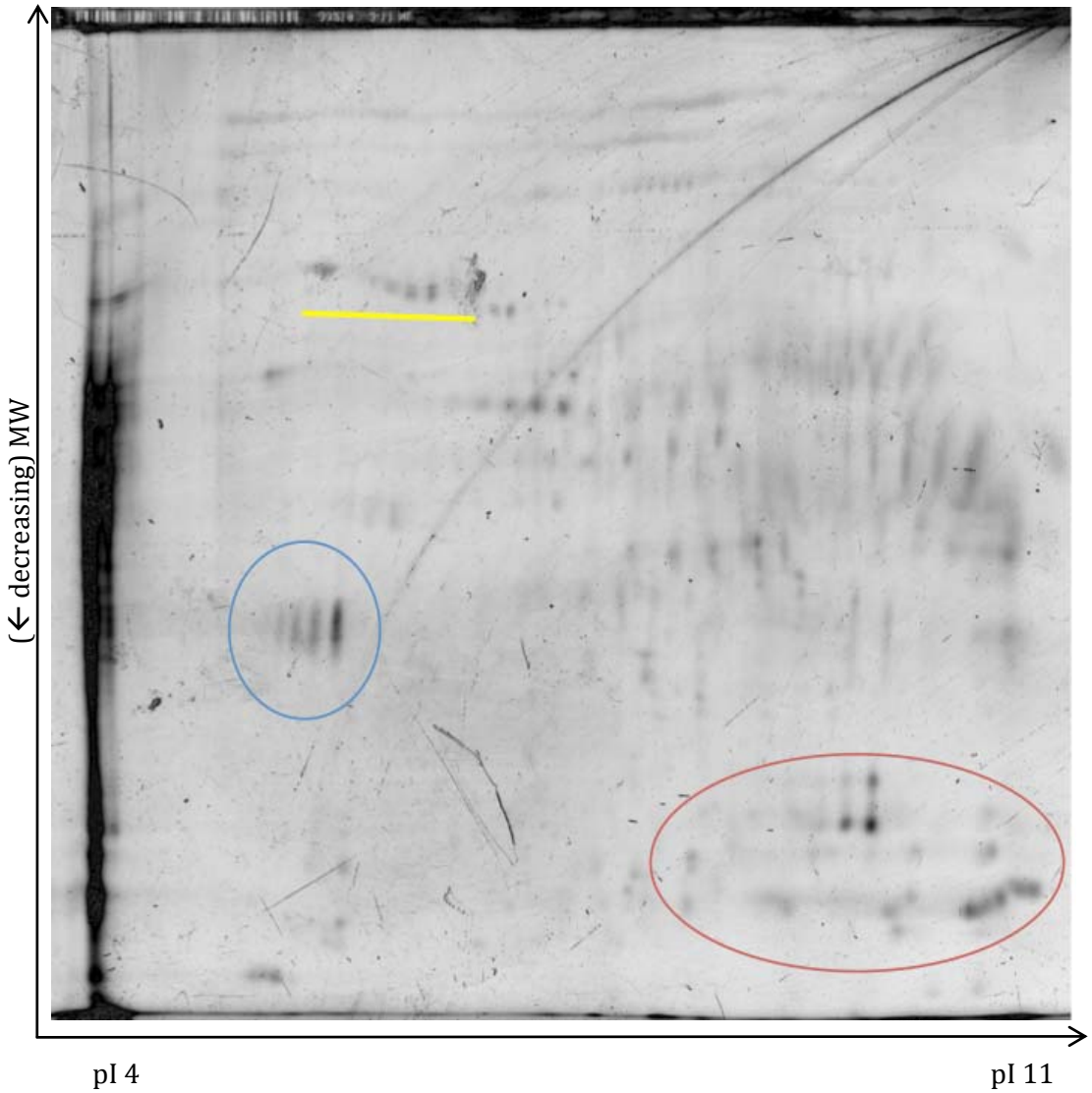

Figure 33. Fluorescence 2D gel image of thiol labeled mouse liver using SO_3-Cy3-Mal

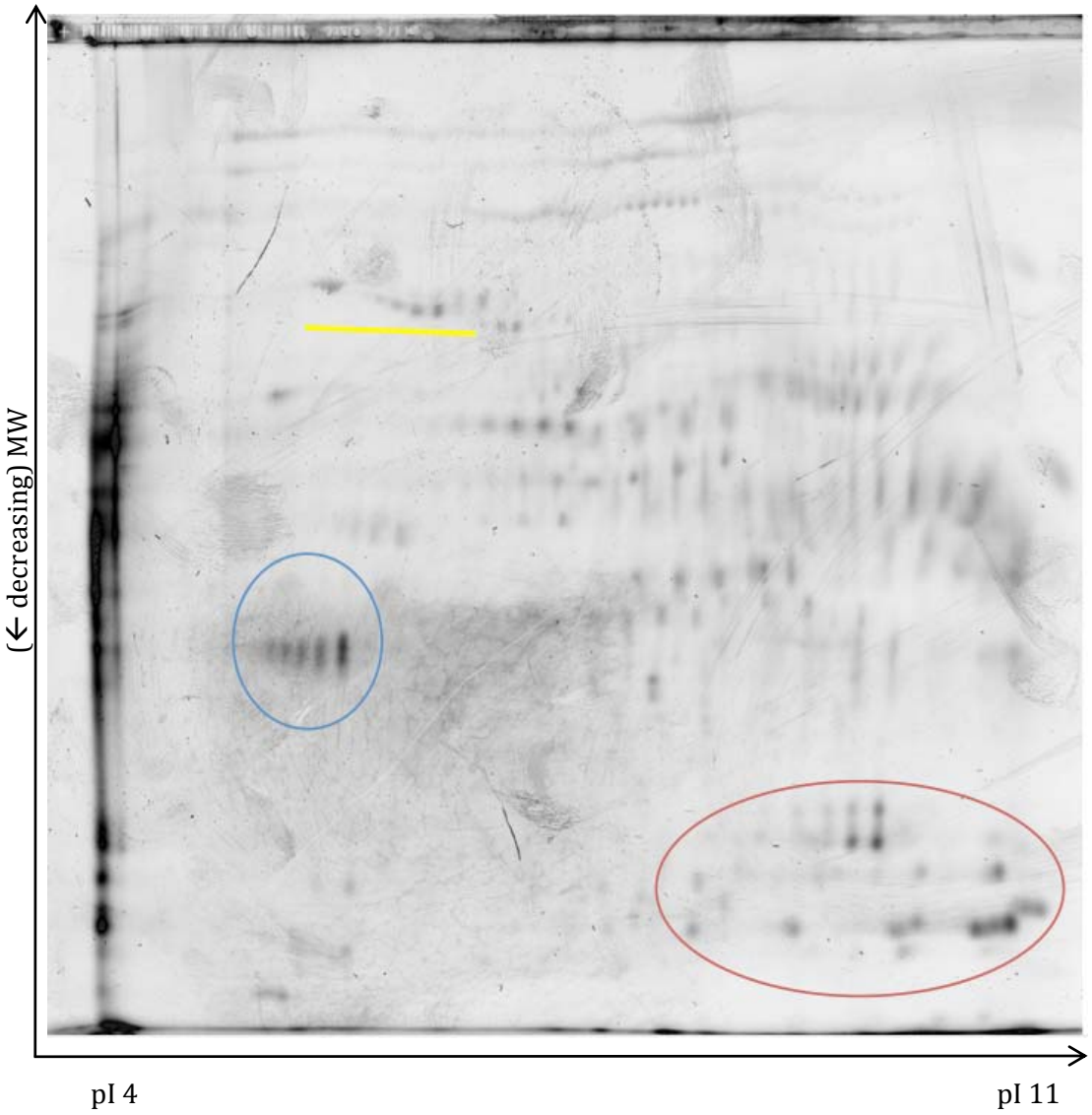

Figure 34. Fluorescence 2D gel image of thiol labeled mouse liver using Z-Cy5-Mal

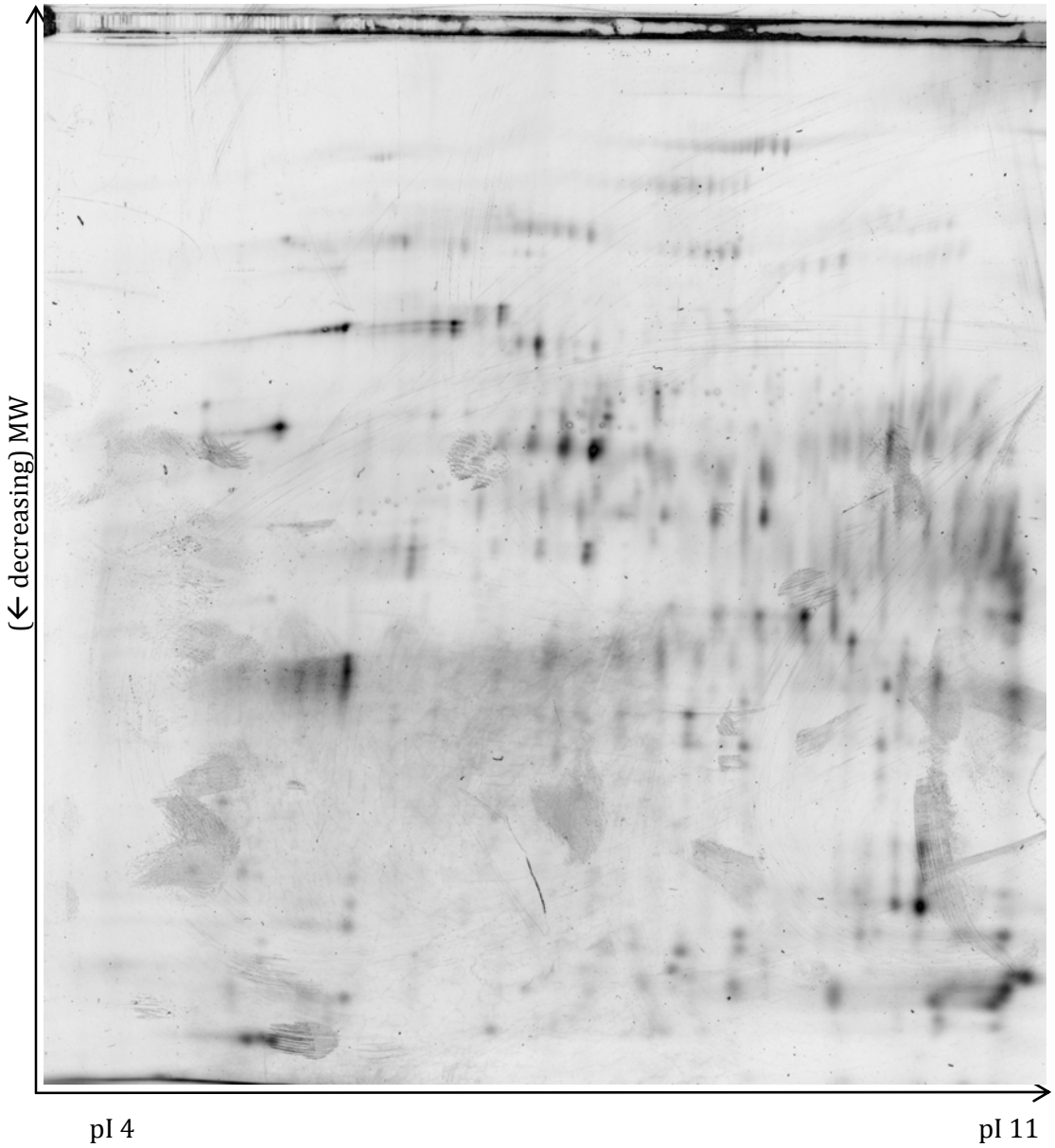

Figure 35. Fluorescence 2D image of thiol labeled mouse liver using SO3-Cy5-Mal

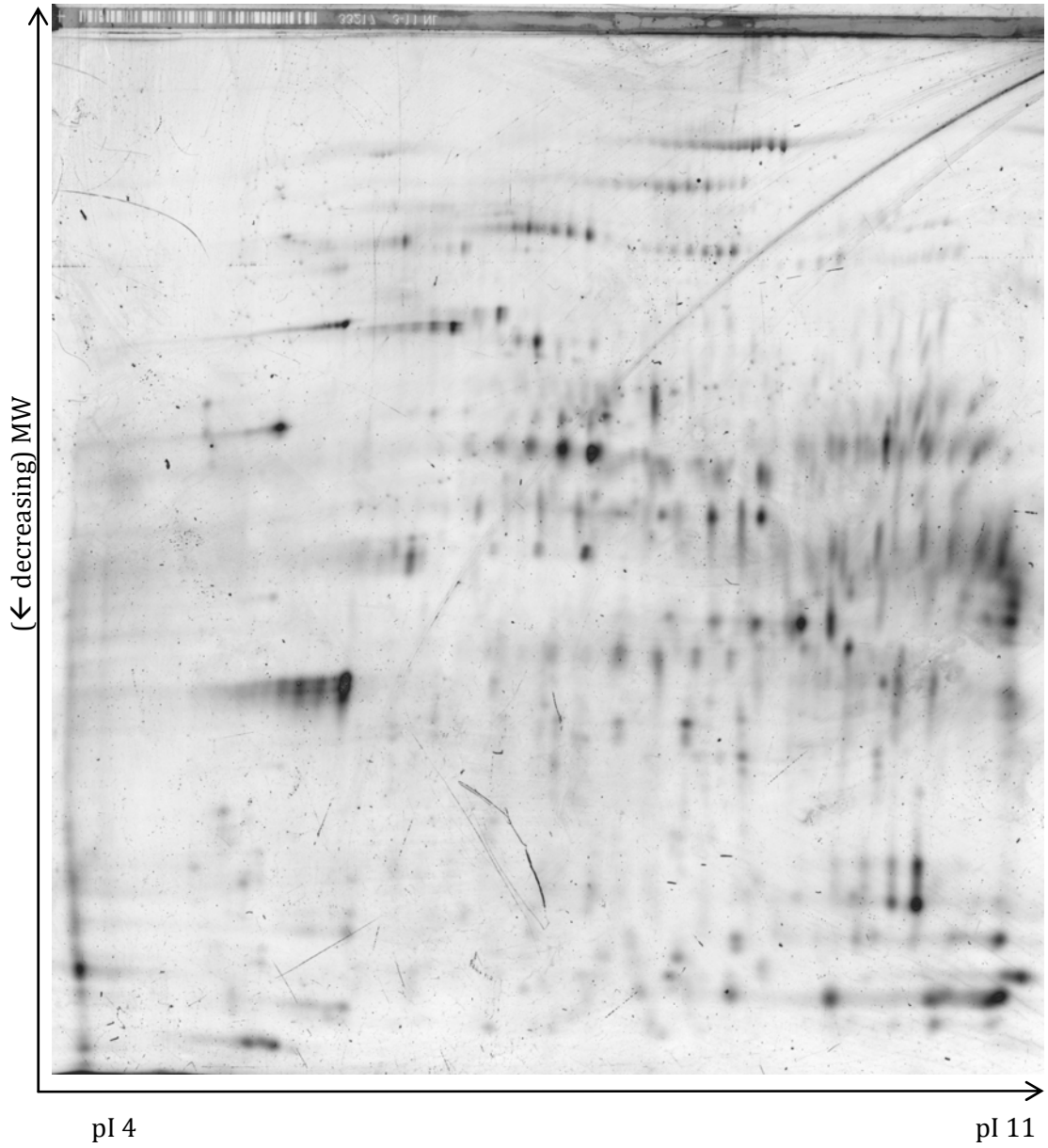

Figure 36. Fluorescence image of thiol labeled mouse liver using Z-Cy3-Mal

CONCLUSIONS

The utility of a novel protein *S*-nitrosothiol detection protocol has been presented; the use of the thiosulfonate switch technique to specifically label protein *S*-nitrosothiols has successfully been demonstrated with single pure proteins (BSA-SNO), a mixture of two pure proteins (BSA/AdhR*-SNO and BSA-SNO/AdhR*-SH) and mouse liver lysates nitrosylated by GSNO. Additionally, the TST protocol has incorporated the use of a zwitterionic cyanine SH probe family of dyes compatible with multiplexing experiments and these three color labeled samples have been analyzed by 2D non-reducing SDS-PAGE gels.

This thesis also demonstrates the use of a biotin switch technique protocol modified to incorporate the Grieco lab's zwitterionic cyanine OPSS and maleimide dyes families. The modified BST has shown similar selectivity for SNO proteins and represents another important analytical protocol for SNO-DIGE.

The use and inability of ascorbate to reduce protein *S*-nitrosothiols has been repeatedly demonstrated in this work and works previous. Ascorbate failed to reduce protein *S*-nitrosothiols in mouse liver lysates in 1D and 2D gels using both the TST and modified BST protocols.

Finally, the synthesis of a second generation zwitterionic cyanine dye with a maleimide reactive motif has been presented and this novel proteomics dye has been demonstrated in comparison to the highly efficient first generation Z-Cy-Mal family in a saturation thiol labeled mouse liver lysate on 2D gels. This second generation maleimide dye set represents a less synthetically challenging family to produce while still mainting

the zwitterionic character that increased the labeling efficiency drastically compared to the original CyDye's.

EXPERIMENTALS

SO_3-Cy3-Mal Synthetic Experimentals

Nuclear magnetic resonance, both proton (^{1}H NMR) and carbon (^{13}C NMR), were recorded using either a 300 MHz Bruker Avance DPX 300 spectrometer or a 500 MHz Bruker Avance DRX 500 spectrometer and all reports are given in parts per million (δ). ^{1}H NMR spectra were determined in a deuterated solvent, and were referenced against the residual solvent signal: methanol-d_4 (CD_3OD) δ 3.31. ^{13}C NMR spectra were determined in deuterated solvents, and were referenced against the residual solvent signal: dimethyl sulfoxide-d6 (DMSO-d6) δ 39.51 and methanol-d_4 (CD_3OD) δ 49.15. FTIR (Fourier transform infrared spectroscopy) spectra was acquired on a JASCO FT/IR 4100; samples were dissolved in dichloromethane, placed onto a sodium chloride salt plate and the solvent was evaporated leaving a thin film of sample or mixed 1:5 with potassium bromide and pressed into a window. Reactions were monitored using reverse phase HPLC utilizing a Shimadzu CBM-2A Prominence Communications Bus Module, Shimadzu SPD-M20A Prominence Diode Array Detector, LC-20AB Prominence Liquid Chromatograph and a Phenomenex Synergi 4µ Polar RP 80Å 250 X 10.00 mm 4 micron column. The mobile phase was always a gradient (A:B) of HPLC grade H_2O: 95% CH_3CN, 5% H_2O containing 0.1% HPLC grade TFA as ion pairing agent. Reverse phase HPLC purification was carried out using a Waters 600 Pump, a Waters 600 Controller and a Waters 2487 Dual λ Absorbance Detector utilizing a preparative reverse phase Phenomenex Synergi 4µ Polar RP 80Å AXIF 250 mm x 21.20 mm 4 micron column. The

mobile phase was always a gradient (A:B) of HPLC grade H_2O: 95% CH_3CN, 5% H_2O containing 0.1% HPLC grade TFA as ion pairing agent. Mass spectra were collected on a Bruker Microtof (ESI-TOF) with an Agilent 1100 HPLC**.** Samples were dissolved in HPLC grade 50:50 water:acetonitrile and run on a 5% to 95% B reverse phase gradient over 4 min before being injected into the ESI source. Unless noted otherwise all reactions were run under argon using anhydrous solvents. All anhydrous solvents were obtained from SIGMA-ALDRICH in Sure/Seal^{TM} bottles. Immobulin NL 3-11 Drystrips and GE Destreak Rehydration Solution was purchased from GE Life Sciences. All other reagents were obtained from SIGMA-ALDRICH and used as received.

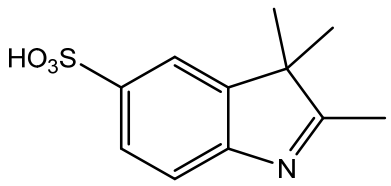

I

2,3,3-trimethyl-3H-indole-5-sulfonic acid (I).

4-Hydrazinobenzenesulfonic acid (4.99g, 26.5mmol, 1.0 eq) was stirred at reflux for 4 h with 8.5 mL of 3-methyl-2-butanone (6.84g, 79.44mmol, 3.0 eq) and 15 mL of glacial acetic acid under an inert atmosphere. The acid was precipitated with cold ethyl acetate and filtered, providing 3.21g, 79% yield, of a pink solid. The pink solid was recrystallized in water: mp 288 - 291 (lit. ref[37] 292-293° C).

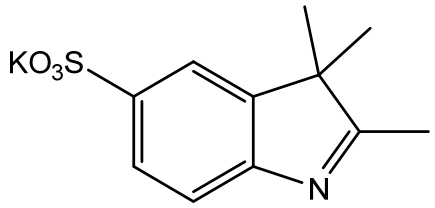

II

Potassium 2,3,3-trimethyl-3H-indole-5-sulfonate (II)

2,3,3-Trimethyl-3H-indole-5-sulfoni acid (3.21g, 13.4mmol, 1 eq) in 50 mL of methanol was deprotonated with a solution of KOH (1.4g, 25mmol, 1.86 eq) in 40mL of n-propanol. The KOH/n-propanol solution was added dropwise to the acid/methanol under an inert atmosphere, which was chilled in ice and stirred overnight. The potassium salt was recovered by removal of the solvent by rotary evaporation followed by lyophilization and yielded 3.7g (99% yield) of the salt as a brown solid with m.p. 291-294 °C (lit. ref[38] 292-293 °C) which was used without further purification.

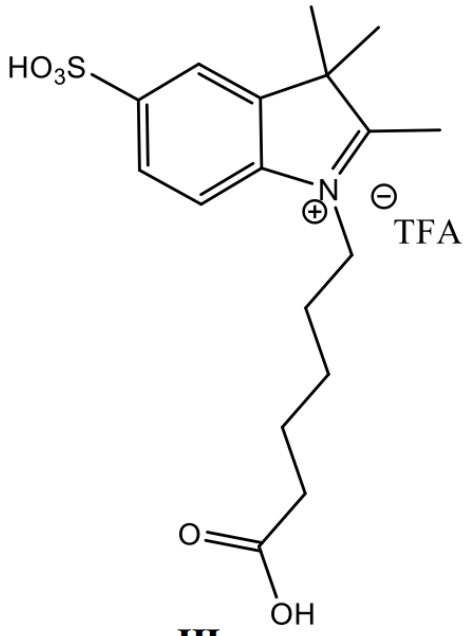

III

1-(5-carboxypentyl)-2,3,3-trimethyl-5-sulfo-3H-indol-1-ium (III).

The suspension of potassium sulfonate indole **II** (106 mg, 0.38 mmol, 1 eq) in 2 mL of 1,2-dichlorobenzene was treated with tetrabutylammonium iodide (382 mg, 1.03 mmol, 2.7 eq). To the stirred suspension was added 6-bromohexanoic acid (131 mg, 0.67 mmol, 1.76 eq). The mixture was stirred for 24 h at 95 °C under an inert atmosphere. The solvent was removed by lyophilization yielding crude product as a yellow powder. Purification via HPLC (30% to 70%B 20 mL/min, 20 min, 280 nm, R_t = 4.5-5.5 min) yielded 84.5 mg (63% yield) of the TFA salt **III** as a yellow powder: FTIR (CH_2Cl_2, cm^{-1}): 3405 (br), 2931, 2866, 1720, 1624, 1469, 1415, 1227, 1170, 1116, 1028, 655; ^{1}H NMR (500 MHz, MeOD) δ 8.10 (m, 1H), 8.01 (m, 1H), 7.90 (m, 1H), 4.50 (q, J = 6.96 Hz, 2H), 2.32 (q, J = 6.48 Hz, 2H), 2.03 – 1.90 (m, 2H), 1.75 – 1.44 (m, 11H). ^{13}C NMR (126 MHz, MeOD) δ 198.39, 175.70, 175.65, 147.06, 142.08, 127.05, 120.89, 115.34,

54.79, 33.03, 27.06, 25.65, 24.01, 21.35. HRMS-EI (m/z): calcd for $C_{17}H_{24}NO_5S^+$ $[M]^+$ 354.1370, found 354.1335.

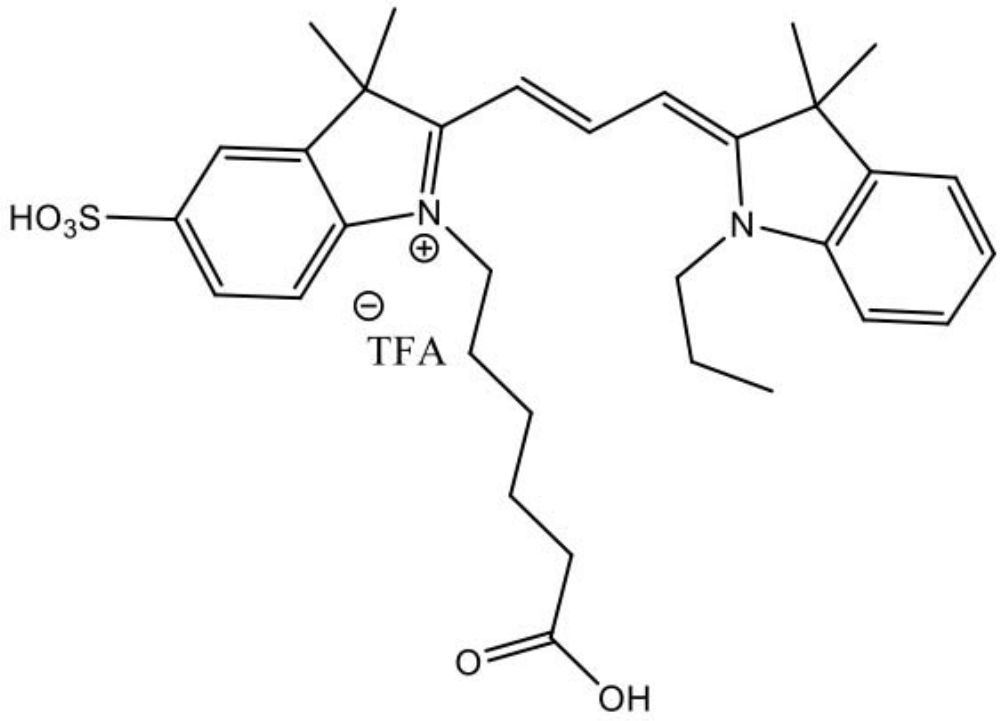

IV

1-(5-carboxypentyl)-2-((E)-3-((Z)-3,3-dimethyl-1-propylindolin-2-ylidene)prop-1-en-1-yl)-3,3-dimethyl-5-sulfo-3H-indol-1-ium (IV.)

A solution of 1-(5-carboxypentyl)-2,3,3-trimethyl-5-sulfo-3H-indol-1-ium salt **III** (50.0mg, 0.11 mmol, 1.0 eq) in acetic anhydride (2.5mL) containing pyridine (2.5mL) was added (*E*)-*N*-(2-(3,3-dimethyl-3H-indol-2-yl)vinyl)-*N*-phenylacetamide (40.0mg, 0.098mmol, 1.12 eq) under an inert atmosphere for 4 h at 110° C. After 4 h at 110° C, the solvent was removed by lyophilization yielding crude product as a deep pink oil. Purification via reverse phase HPLC (30 to 70% B, 20 mL/min, 30 min, 530nm, R_t = 19-

21 min) provided 28.9 mg (44.5% yield) of the TFA salt **IV** as a deep pink powder: FTIR (CH_2Cl_2, cm^{-1}): 3441 (br), 2927, 2858, 1698, 1558, 1437, 1368, 1236, 1190, 1114, 1034, 931; ^1H NMR (300 MHz, CD_3OD): δ 8.54 (t, *J* = 13.4 Hz, 1H), 7.91 (s, 1H), 7.87 (d, *J* = 7.4 Hz, 1H), 7.56 (d, *J* = 7.4 Hz, 1H), 7.29-7.48 (m, 4H), 6.54 (d, *J* = 13.4 Hz, 1H), 6.44 (d, *J* =13.4 Hz, 1H) 4.13 (br m, 4H), 2.30 (t, *J* = 7.2 Hz, 2H), 1.20-1.93 (m, 17H), 1.06 (t, *J* = 7.4 Hz, 3H). ^{13}C NMR (75 MHz, CD_3OD) δ 175.81, 175.67, 174.35, 151.04, 143.47, 142.18, 141.91, 141.09, 140.52, 128.66, 126.83, 125.81, 122.21, 120.03, 111.52, 110.36, 103.48, 102.38, 45.47, 43.74, 33.21, 29.39, 29.05, 26.96, 26.85, 26.67, 25.88, 24.31, 20.63, 10.08. HRMS-EI (m/z): calcd for $C_{32}H_{41}N_2O_5S^+$ $[M]^+$ 565.2731, found 565.2662.

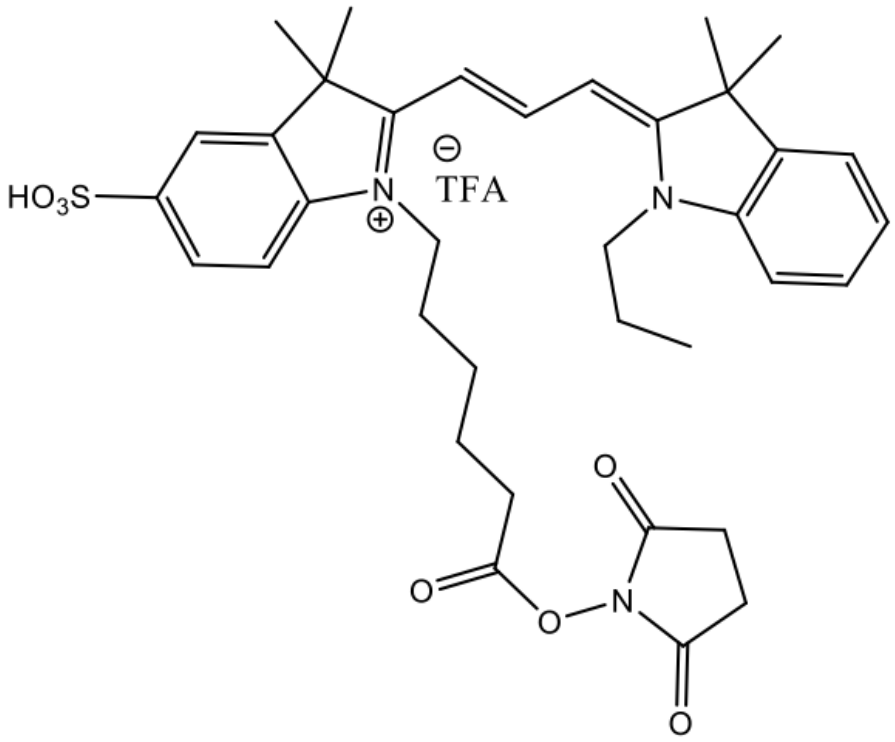

V

2-((E)-3-((Z)-3,3-dimethyl-1-propylindolin-2-ylidene)prop-1-en-1-yl)-1-(6-((2,5-dioxopyrrolidin-1-yl)oxy)-6-oxohexyl)-3,3-dimethyl-5-sulfo-3H-indol-1-ium (V).

To a solution of compound **IV** (24.5 mg, 0.037 mmol, 1.0 eq) in *N,N*-dimethylformamide (3.0 mL) under an inert atmosphere at ambient temperature was added *N*-hydroxysuccinimide (39.8 mg, 0.346 mmol, 9.3 eq) followed by the addition of *N,N*-diisopropylcarbodiimide (42 μL, 0.268 mmol, 7.2 eq). The mixture was stirred for 18 h. The solvent was removed by lyophilization yielding the crude product as a deep pink oil. Purification was performed via reverse phase HPLC (30% to 70% B, 20mL/min, 30min, 530nm, R_t = 19-21min) and provided 14.5 mg (50.5% yield) of the TFA salt **V** as a deep pink film. FTIR (KBr, cm^{-1}): 3402 (br), 2923, 2852, 1654, 1638, 1560, 1460, 1395, 1120, 1094, 1028, 620; ^{1}H NMR (500 MHz, CD_3OD): δ 8.54 (t, *J* = 13.4 Hz, 1H), 7.9 (s, 1H), 7.86 (d, *J* = 7.5 Hz, 2H), 7.56 (d, *J* = 7.5 Hz, 1H), 7.30 – 7.46 (m, 4H), 6.54 (d, *J* =13.4 Hz, 1H), 6.44 (d, *J*= 13.4 Hz, 1H) 4.14 (br m, 4H), 2.79 (br s, 4H), 2.65 (t, *J* = 7.0 Hz, 2H), 1.72 – 1.93 (m, 20H), 1.59 (m, 2H), 1.06 (t, *J* = 7.3 Hz, 3H). ^{13}C NMR (126 MHz, MeOD) δ 175.61, 171.13, 151.03, 143.41, 142.21, 141.88, 141.04, 140.51, 134.04, 128.61, 126.79, 125.76, 122.17, 120.00, 111.43, 110.39, 103.32, 102.33, 45.43, 43.72, 37.39, 37.06, 35.19, 35.13, 29.34, 26.90, 26.80, 26.63, 25.79, 24.84, 20.57, 10.03.HRMS-EI (m/z): calcd for $C_{36}H_{44}N_3O_7S^+$ $[M]^+$ 662.2894, found 662.2873.

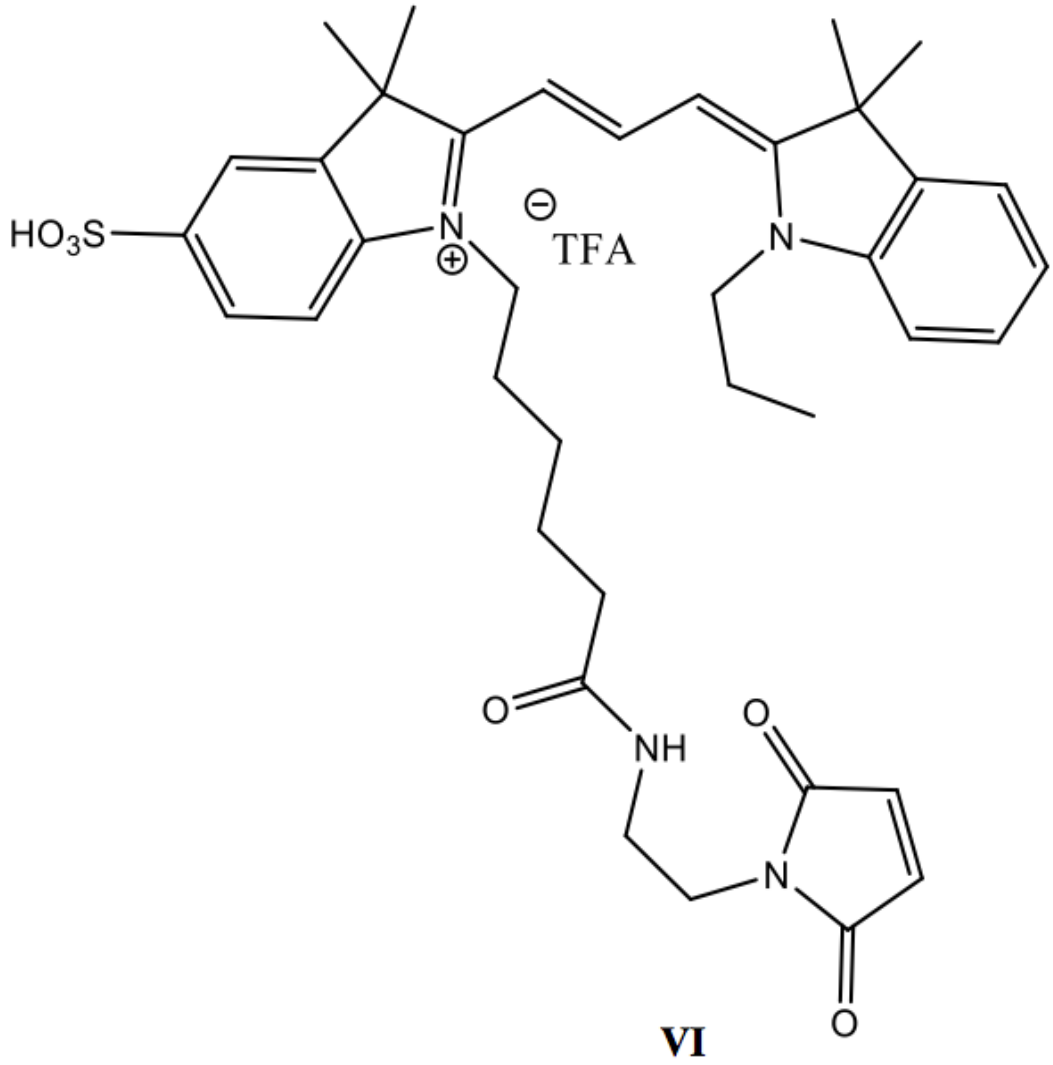

VI

2-((E)-3-((Z)-3,3-dimethyl-1-propylindolin-2-ylidene)prop-1-en-1-yl)-1-(6-((2-(2,5-dioxo-2,5-dihydro-1H-pyrrol-1-yl)ethyl)amino)-6-oxohexyl)-3,3-dimethyl-5-sulfo-3H-indol-1-ium (VI)

To a solution of compound **V** (9.0mg, 11.86 µmol, 1 eq) in *N,N*-dimethylformamide (2 mL) containing *N*-Methylmorpholine (25.8 µg, 237.2 µmol, 20 eq) was added the trifluoroacetate salt of *N*-(2-aminoethyl)maleimide (15.0 mg, 59.3 µmol, 5 eq) . After 20 h at ambient temperature in the dark, the solvent was removed by

lyophilization yielding crude product as a deep pink powder. Purification was performed via reverse phase HPLC (30% to 70% B, 20mL/min, 30min, 530nm, R_t = 16-18 min) and provided 4.5 mg (48% yield) of the TFA salt **VI** as a deep pink powder: FTIR (CH_2Cl_2, cm^{-1}): 3410 (br), 2963, 2926, 2851, 1705, 1650, 1560, 1440, 1415, 1261, 1100, 1023, 800; ^1H NMR (300 MHz, CD_3OD) δ 8.54 (t, *J* = 13.4 Hz, 1H), 7.90 (s, 1H), 7.87 (d, *J* = 7.4 Hz, 1H), 7.56 (d, *J* = 7.4 Hz, 1H), 7.28 – 7.49 (m, 4H), 6.78 (s, 2H), 6.53 (d, *J* = 13.4 Hz, 1H), 6.45 (d, *J* = 13.4 Hz, 1H) 4.13 (m, *J* = 4H), 3.57 (br t, *J* = 7.2 Hz, 2H), 2.11 (t, *J* = 7.2 Hz, 2H), 1.20-1.94 (m, 17H), 1.06 (t, *J* = 7.4 Hz, 3H). ^{13}C NMR (126 MHz, CD_3OD) δ 151.03, 134.04, 128.60, 126.79, 125.75, 122.17, 120.00, 111.42, 110.39, 103.28, 102.31, 45.41, 43.71, 37.39, 37.06, 35.12, 26.90, 26.80, 26.62, 25.78, 24.83, 20.57, 10.02. HRMS-EI (m/z): calcd for $C_{38}H_{47}N_4O_6S^+$ $[M]^+$ 687.3211, found 687.3150.

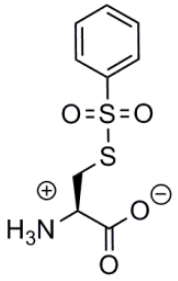

***S*-phenylsulfonylcysteine (SPSC).** The synthesis of **SPSC** was performed by modifying a literature procedure.[35] To a stirred solution of L-cysteine (240 mg, 2.0 mmol) in 2 N HCl (2 mL) was slowly added a solution of $NaNO_2$ (138 mg, 2.0 mmol) in water (0.5 mL). After 40 min at 5 ^oC the deep red solution was treated with a solution of $PhSO_2Na$ (650 mg, 4.0 mmol) in water (4 mL) and stirred for 1 h at 5 ^oC and 4 h at rt.

The precipitate was filtered and washed with water (2 x 4 mL), acetone (2 x 3 mL) and ether (2 x 3 mL). Drying by lyophilization provided 332 mg of SPSC as a white solid (66% yield): ^{1}H NMR (300 MHz, d-DMSO): δ 3.30-3.15 (m, 2H), 3.35-3.41 (m, 2H), 7,66-7.80 (m, 2H), 7.91 (d, 2H, J= 7.7 Hz); ^{13}C NMR (125 MHz, CD_3OD,): δ 36.36, 53.91, 128.50, 131.08, 135.90, 169.79; HRMS-EI (m/z): calcd for $C_9H_{11}NO_4S_2$ $[M + H]^+$ 262.0202, found 262.0227.

Protein Purification, Switch Technique and Gel Analysis Protocols

Wild type mouse liver samples were received on dry ice from E.E. Schmidt. After being stored at -80 ^{o}C, samples were homogenized with a mortar and pestle, chilled with dry ice in ethanol. Homogenized liver samples were aliquoted in 0.5g to 1.5g size into 1.6 mL eppindorf tubes and stored at -80 ^{o}C.

When lysing the liver samples, special care was taken to preserve the thiol-disulfide status in order to prevent labeling of thiols that are normally in an oxidized state in the cell. To achieve this, homogenized samples were diluted in pH 4 or 4.5 ammonium formate buffer. While the TST protocol is most efficient at pH 4, protein recovery from lysis at pH 4 is normally very low, so the increase to pH 4.5 allows for much great protein recovery while still not compromising the redox state of the thiol proteome. Samples were diluted in 1 mL of the buffer and vortexed for 10-20 min, after which time they were lysed with an ultrasonicator at 30% power, 60 pulses for 10 min, on ice. The resulting mixtures were spun down 3 times at 14,000 XG for 15 min and the supernatants

were collected. Protein concentration was determined by Bradford concentration assays (BCA.) The concentration of protein ranged from 40-75 mg/mL and the samples were aliquoted in 5 uL fractions and frozen.

S-Nitrosoglutathione (GSNO) was prepared by mixing equivalent molar concentrations of glutathione and sodium nitrite in 2.0 M HCl in the dark for 40 min. After precipitating the pink GSNO out of solution with cold acetone, the crude product was washed with water, acetone and diethyl ether three times each. The pink powder was lyophilized and stored in the dark at -4^{o} C. Liver lysate samples were nitrosylated in pH 8 HEN buffer with 10 uL of 10 mM GSNO (also in pH 8 HEN) for 1 h, in the dark, at ambient temperature. Excess GSNO was removed by purification over micro-biospin 6 columns. For BST experiments, pH 8 HEN preequilibrated columns were used and for TST, pH 4 or 4.5 ammonium formate (NH_4HCO_2) were used. BSA-SNO was prepared by reacting BSA (reduced with β-mercaptoethanol and purified with pH 8 HEN sephadex G-25 columns) with *S*-nitrosocysteine as previously reported. This procedure was also used for ADHR-SNO and Papain-SNO preparation.

Thiosulfonate Switch Protocol

Mouse liver lysate aliquots (5 µL, 40-75 mg/mL, pH 4.5 ammonium formate buffer) were diluted with 50 µL of pH 8.0 HEN buffer and nitrosylated with 20 µL (10 mM) GSNO (3.4 mg GSNO in 1 mL pH 8.0 HEN) for 1 h, in the dark, at ambient temperature. Excess GSNO was removed from the samples by spinning them over preequilibrated pH 4.0 MicroBiospin 6 columns. Columns were buffer exchanged by

rinsing them 3 times with 500 µL of pH 4.0 ammonium formate buffer. For a UV knockout control, one sample was subjected to 312 nm UV light for 10 min after the MicroBiospin 6 columns. Samples were blocked with 16 µL 1mM SPSC (2.6 mg SPSC in 10 mL pH 4.0 ammonium formate) for 1 h, dark, ambient temperature. SNO residues were trapped with 5 µL 0.5 M sodium benzene sulfinate (8.2 mg $PhSO_2Na$ in 100 µL pH 4.0 ammonium formate buffer) for 30 min, in the dark, at ambient temperature. Before dye was added to the samples, an aliquot (5 µL) was removed for BCA analysis. Labeling was achieved by the addition of 0.8 nmol of Z-Cy-SH dye (2 µL of 0.4 mM dye solution in DMF) for 10 min, in the dark, at ambient temperature. Excess dye was quenched with the addition of 80 nmol of MMTS (4 µL of 20 mM MMTS in DMF.) Samples were either frozen at -80 °C or run immediately on non-reducing SDS-PAGE gels.

Biotin Switch Assay Modified Protocol

Mouse liver lysate aliquots (5 µL, 40-75 mg/mL, pH 4.5 ammonium formate buffer) were diluted with 50 µL of pH 8.0 HEN buffer and nitrosylated with 20 µL (10 mM) GSNO (3.4 mg GSNO in 1 mL of pH 8.0 HEN) for 1 h, in the dark, at ambient temperature. Excess GSNO was removed from the samples by spinning them over preequilibrated pH 8.0 MicroBiospin 6 columns. Columns were buffer exchanged by rinsing them 3 times with 500 µL of pH 8.0 HEN buffer. For a UV knockout control, one sample was subjected to 312 nm UV light for 10 min after the MicroBiospin 6 columns. Samples were diluted in 1.8 mL of pH 8.0 HEN buffer and 200 µL 25% SDS (in pH 8.0 HEN) and blocked with MMTS (20 µL of 10% MMTS in DMF, 20 µmol) for 20 min, in

the dark, at 37 °C. The blocked proteins were precipitated in cold acetone for 2 h, in the dark, at -4 °C. After spinning the samples for 5 min at 5,000 XG, pelleted protein was resuspended in 100 µL pH 8.0 HENS buffer. Before the dye and ascorbate were added, an aliquot (5 µL) was removed for BCA analysis. Labeling was achieved by the addition of 8 nmol of Z-Cy-OPSS or Z-Cy-Mal (2 µL (4mM) in DMF) and 30 µL (200 mM) sodium ascorbate (in pH 8.0 HEN buffer) for 1 h, in the dark, at ambient temperature. Samples were either frozen at -80 °C or run immediately on non-reducing SDS-PAGE gels.

IEF and DIGE Experiments

For 2D gel experiments, samples were first combined and diluted to a final volume of 450 µL with IEF buffer. Samples were focused on GE Immobulin Drystrips NL 3-11 using the following voltage protocol;

Step 1: 50V, Step-n-hold for 12 h
Step 2: 500V, Step-n-hold for 1h
Step 3: 1000V, gradient for 1h
Step 4: 3000V, gradient for 1h
Step 5: 5000V, gradient for 1h
Step 6: 8000V, gradient for 1h
Step 7: 8000V, Step-n-hold until 35,000 Vhr (40,000-50,000 Vhr total)

After the strips had finished focusing, they were washed with SDS equilibration buffer (3 mL per gel) without the inclusion of IAM or DTT. The strips were loaded onto 14% acrylamide 2D non-reducing gels and sealed with sealing buffer. Gels were run at a constant wattage of 2W/gel until the bromophenyl blue dye front reached to within one

inch of the bottom of the gel. After the second dimension focusing had been completed, gels were immediately scanned on the Typhoon scanner at appropriate wavelengths.

Typhoon Gel Imaging

Gels were imaged using the GE Typhoon Trio scanner at the following excitation/emission wavelengths (nm); Cy2 (485/500), Cy3 (548/564), and Cy5 (642/663). Gels were scanned at 100 micron resolution and a photomultiplier tube voltage of 600V. Scanned images were processed and spot volumes were calculated using the NIH freeware ImageJ.

Buffer List

pH 4.0 Ammonium Formate: 100 mM NH_4HCO_2, 1 mM EDTA, pH 4.0

pH 4.5 Ammonium Formate: 100 mM NH_4HCO_2, 1 mM EDTA, pH 4.5

pH 8.0 HEN: 100 mM HEPES, 1mM EDTA, 0.1 mM neocuproine, pH 8.0

pH 8.0 HENS: 100 mM HEPES, 1 mM EDTA, 0.1 mM neocuproine, 1% SDS (w/v)

IEF buffer: 7 M Urea, 2 M Thiourea, 4% CHAPS, 0.1% ASB-14, 0.05% IPG Ampholytes

SDS equilibration buffer: 50 mM Tris-Cl, 6 M Urea, 30% glycerol (v/v), 2% SDS (w/v), bromophenyl blue (trace), pH 8.8

Saturation Labeling Buffer: 7 M urea, 2 M thiourea, 4% CHAPS, pH 8.0

Saturation Labeling Stopping Buffer: 7 M urea, 2 M thiourea, 4% CHAPS, 0.5% IPG ampholytes, 0.01% bromopehnyl blue

REFERENCES CITED

[1] Poole, L. B., The basics of thiols and cysteines in redox biology and chemistry. *Free Radical Biology and Medicine* **2015,** *80* (0), 148-157.

[2] Chung, H. S.; Wang, S.-B.; Venkatraman, V.; Murray, C. I.; Van Eyk, J. E., Cysteine Oxidative Posttranslational Modifications: Emerging Regulation in the Cardiovascular System. *Circulation Research* **2013,** *112* (2), 382-392.

[3] Timerghazin, Q. K.; Peslherbe, G. H.; English, A. M., Resonance Description of S-Nitrosothiols: Insights into Reactivity. *Org Lett.* **2007,** *9* (16), 3049-3052.

[4] Hughes, M. N., Relationships between nitric oxide, nitroxyl ion, nitrosonium cation and peroxynitrite. *Biochimica et Biophysica Acta (BBA) - Bioenergetics* **1999,** *1411* (2–3), 263-272.

[5] Arnelle, D. R.; Stamler, J. S., NO+, NO., and NO− Donation by S-Nitrosothiols: Implications for Regulation of Physiological Functions by S-Nitrosylation and Acceleration of Disulfide Formation. *Archives of Biochemistry and Biophysics* **1995,** *318* (2), 279-285.

[6] Gaston, B., Singel, D.J., Doctor, A., Stamler, J.S. S-nitrosylation signaling in cell biology. *Mol. Interven.* **2003**, *3*, 253-262.

[7] Xian, M., Chen, X., Liu, Z., Wang, K., Wang, P.G. Inhibition of Papain by S-Nitrosothiols. *J. Biol. Chem.* **2000,** *275,* 20467-20473.

[8] Chanvorachote, P., Nimmannit, U., Wang, L.; Stehlik, C., Lu, B., Azad, N., Rojanasakul, Y. Nitric oxide negatively regulates Fas CD95-induced apoptosis through inhibition of ubiquitin–proteasome-mediated degradation of FLICE inhibitory protein. *J. Biol. Chem*. **2005**, *280,* 42044–42050.

[9] Diesen, D. L., Hess, D. T., Stamler, J. S. Hypoxic Vasodilation by Red Blood Cells: Evidence for an S-Nitrosothiol–Based Signal. *Circulation Research* **2008,** *103* (5), 545-553.

[10] Mollace, V., Muscoli, C., Masini, E., Cuzzocrea, S., Salvemini, D. Modulation of Prostaglandin Biosynthesis by Nitric Oxide and Nitric Oxide Donors. *Pharmacol. Rev.* **2005**, *57,* 217-252.

[11] Tanaka, Y., Igimi, S., Amano, F. Inhibition of Prostaglandin Synthesis by Nitric Oxide in RAW 264.7 Macrophages. *Arch. Biochem. Biophys.* **2001,** *391* (12), 207-217.

[12] Lipton, S. A., Choi, Y. B., Pan, Z. H., Lei, S. Z., Chen, H. S., Sucher, N. J., Loscalzo, J., Singel, D. J., Stamler, J. S. A redox-based mechanism for the neuroprotective and neurodestructive effects of nitric oxide and related nitroso-compounds. *Nature.* **1993**, *364*, 626–632.

[13] Mustafa, A. K., Kumar, M., Selvakumar, B., Ho, G. P., Ehmsen, J. T., Barrow, R. K., Amzel, L. M., Snyder, S. H. Nitric oxide S-nitrosylates serine racemase, mediating feedback inhibition of D-serine formation. *Proc. Natl. Acad. Sci*. **2007**, *104*, 2950–2955.

[14] Whalen, E. J., Foster, M. W., Matsumoto, A., Ozawa, K., Violin, J. D., Que, L. G., Nelson, C. D., Benhar, M., Keys, J. R., Rockman, H. A., Koch, W. J., Daaka, Y., Lefkowitz, R. J., Stamler, J. S. Regulation of beta-adrenergic receptor signaling by S-nitrosylation of G-protein-coupled receptor kinase 2. *Cell,* **2007**, *129,* 511–522.

[15] Kokkola, T., Savinainen, J. R., Monkkonen, K. S., Retamal, M. D., Laitinen, J. T. S-nitrosothiols modulate G protein-coupled receptor signaling in a reversible and highly receptor-specific manner. *BMC Cell Biol*, **2005**, *6,* 21.

[16] Uehara, T.; Nakamura, T.; Yao, D.; Shi, Z. Q.; Gu, Z.; Ma, Y.; Masliah, E.; Nomura, Y.; Lipton, S. A. S-nitrosylated protein-disulphide isomerase links protein misfolding to neurodegeneration. *Nature,* **2006**, *441*, 513–517.

[17] M.W. Foster, T.J. McMahon, J.S. Stamler, S-nitrosylation in health and disease, *Trends Mol. Med.* **2003**, *9,* 160–168.

[18] M.W. Foster, D.T. Hess, J.S. Stamler, Protein S-nitrosylation in health and disease: a current perspective, *Trends Mol. Med.* **2009,** *15* 391–404.

[19] Thomsen, L. L.; Scott, J. M.; Topley, P.; Knowles, R. G.; Keerie, A. J.; Frend, A. J. Selective inhibition of inducible nitric oxide synthase inhibits tumor growth in vivo: studies with 1400W, a novel inhibitor. *Cancer Res.* **1997,** *57,* 3300–3304.

[20] Reeves, B. D., Joshi, N., Campanello, G. C., Hilmer, J. K., Chetia, L., Vance, J. A., Reinschmidt, J. N., Miller, C. G., Giedroc, D. P., Dratz, E. A., Singel, D. J., Grieco, P. A. Conversion of S-phenylsulfonylcysteine residues to mixed disulfides at pH 4.0: utility in protein thiol blocking and in protein-S-nitrosothiol detection. *Org. Biomol. Chem.* **2014,** *12* (40), 7942-7956.

[21] Reeves, B.D., Hilmer, J.K., Mellmann, L., Hartzheim, M., Poffenberger, K., Johnson, K., Joshi, N., Singel, D.J., Grieco, P.A. Selective trapping of SNO-BSA and GSNO by benzenesulfinic acid sodium salt: mechanistic study of thiosulphonate formation and feasibility as a protein S-nitrosothiol detection strategy. *Tet Lett*., **2013**, *54*, 5707–5710

[22] Jaffrey, S. R., Erdjument-Bromage, H., Ferris, C. D., Tempst, P., Snyder, S. H. Protein S-nitrosylation: a physiological signal for neuronal nitric oxide. *Nat. Cell Biol*.**2001,** *3*, 193–197.

[23] Landmesser, U.; Dikalov, S.; Price, S. R.; McCann, L.; Fukai, T.; Holland, S. M.; Mitch, W. E.; Harrison, D. G., Oxidation of tetrahydrobiopterin leads to uncoupling of endothelial cell nitric oxide synthase in hypertension. *Journal of Clinical Investigation* **2003,** *111* (8), 1201-1209.

[24] DiGirolamo, G. Farina, M., Riberio, M.L., Ogando, D., Aisemberg, J., de los Santos, A.R., Marti, M.L., Franchi, A.M. Effects of cyclooxygenase inhibitor pretreatment on nitric oxide production, nNOS and iNOS expression in rat cerebellum. *Br. J. Pharmacol.* **2003,** *139* (6), 1164-1170.

[25] Jayachandran, M., Hayashi, T., Sumi, D., Thakur, N.K., Kano, H., Ignarro, L.J., Iguchi, A. Up-regulation of endothelial nitric oxide synthase through beta(2)-adrenergic receptor--the role of a beta-blocker with NO-releasing action. *Biochem Biophys Res Commun.* **2001,** *280*, (3), 589-594.

[26] Costa, V., Quintanilha, A., Moradas-Ferreira, P. Protein oxidation, repair mechanisms and proteolysis in Saccharomyces cerevisiae. *IUBMB Life* **2007,** *59* (4-5), 293-298.

[27] National Cancer Institute. Office of Cancer Clinical Proteomics Research – What is Proteomics? http://proteomics.cancer.gov/whatisproteomics (accessed May 29, 2015).

[28] Unlu, M., Morgan, M. E., Minden, J. S., Difference gel electrophoresis: a single gel method for detecting changes in protein extracts. *Electrophoresis* **1997**, *18*, 2071–2077.

[29] Epstein, M. G.; Reeves, B. D.; Maaty, W. S.; Fouchard, D.; Dratz, E. A.; Bothner, B.; Grieco, P. A. Enhanced Sensitivity Employing Zwitterionic and pI Balancing Dyes (Z-CyDyes) Optimized for 2D-Gel Electrophoresis Based on Side Chain Modifications of CyDye Fluorophores. New Tools For Use in Proteomics and Diagnostics. *Bioconjugate Chem*. **2013**, *24*, (9), 1552-1561.

[30] Hetrick, E. M.; Schoenfisch, M. H., Analytical Chemistry of Nitric Oxide. *Annual review of analytical chemistry (Palo Alto, Calif.)* **2009,** *2*, 409-433.

[31] Saville, B., A Scheme for the colorimetric determination of microgram amounts of thiols. *Analyst*, **1958**. *83*, 670-72.

[32] Doctor, A.; Gaston, B., Detecting physiologic fluctuations in the *S*-nitrosohemoglobin micropopulation: triiodide versus 3C. *Blood.* **2006**; *108*, 3225-3227.

[33] Zhang, Y., Keszler, A., Broniowska, K. A., Hogg, N. Characterization and application of the biotin-switch assay for the identification of S-nitrosated proteins. *Free Radical Biology and Medicine* **2005,** *38* (7), 874-881.

[34] Kirsch, M., Buscher, A.-M., Aker, S., Schulz, R., de Groot, H. New insights into the S-nitrosothiol-ascorbate reaction. The formation of nitroxyl. *Organic & Biomolecular Chemistry* **2009,** *7* (9), 1954-1962.

[35] Forrester, M. T., Foster, M. W., Benhar, M., Stamler, J. S. Detection of Protein S-Nitrosylation with the Biotin Switch Technique. *Free radical biology & medicine* **2009,** *46* (2), 119-126.

[36] Doulias, P.-T.; Greene, J. L.; Greco, T. M.; Tenopoulou, M.; Seeholzer, S. H.; Dunbrack, R. L.; Ischiropoulos, H., Structural profiling of endogenous S-nitrosocysteine residues reveals unique features that accommodate diverse mechanisms for protein S-nitrosylation. *Proceedings of the National Academy of Sciences,* **2010,** *107* (39), 16958-16963.

[37] Hart, T. W. Some observations concerning the S-nitroso and S-phenylsulphonyl derivatives of L-cysteine and glutathione. *Tetrahedron Letters* **1985,** *26* (16), 2013-2016.

[38] Hart, T. W., Vine, M. B., Walden, N. R. Thiolsulphonate derivatives of amino acids. *Tetrahedron Letters* **1985,** *26* (32), 3879-3882.

[39] Choi, H. S.; Nasr, K.; Alyabyev, S.; Feith, D.; Lee, J. H.; Kim, S. H.; Ashitate, Y.; Hyun, H.; Patonay, G.; Strekowski, L.; Henary, M.; Frangioni, J. V., Synthesis and In Vivo Fate of Zwitterionic Near-Infrared Fluorophores. *Angewandte Chemie International Edition* **2011,** *50* (28), 6258-6263.

[40] Lopalco, M.; Koini, E. N.; Cho, J. K.; Bradley, M., Catch and release microwave mediated synthesis of cyanine dyes. *Organic & Biomolecular Chemistry* **2009,** *7* (5), 856-859.